2. Taneja, V., and C. S. David. 2001. Lessons from animal models for human autoimmune diseases. *Nat. Immunol.* 2: 781–784.
3. Diaz, L. A., H. Ratrie, III, W. S. Saunders, S. Futamura, H. L. Squiquera, G. J. Anhalt, and G. J. Giudice. 1990. Isolation of a human epidermal cDNA corresponding to the 180-kD autoantigen recognized by bullous pemphigoid and herpes gestationis sera. Immunolocalization of this protein to the hemidesmosome. *J. Clin. Invest.* 86: 1088–1094.
4. Giudice, G. J., D. J. Emery, and L. A. Diaz. 1992. Cloning and primary structural analysis of the bullous pemphigoid autoantigen BP180. *J. Invest. Dermatol.* 99: 243–250.
5. Hopkinson, S. B., K. S. Riddelle, and J. C. Jones. 1992. Cytoplasmic domain of the 180-kD bullous pemphigoid antigen, a hemidesmosomal component: molecular and cell biologic characterization. *J. Invest. Dermatol.* 99: 264–270.
6. Bédane, C., J. R. McMillan, S. D. Balding, P. Bernard, C. Prost, J. M. Bonnetblanc, L. A. Diaz, R. A. Eady, and G. J. Giudice. 1997. Bullous pemphigoid and cicatricial pemphigoid autoantibodies react with ultrastructurally separable epitopes on the BP180 ectodomain: evidence that BP180 spans the lamina lucida. *J. Invest. Dermatol.* 108: 901–907.
7. Ishiko, A., H. Shimizu, A. Kikuchi, T. Ebihara, T. Hashimoto, and T. Nishikawa. 1993. Human autoantibodies against the 230-kD bullous pemphigoid antigen (BPAG1) bind only to the intracellular domain of the hemidesmosome, whereas those against the 180-kD bullous pemphigoid antigen (BPAG2) bind along the plasma membrane of the hemidesmosome in normal human and swine skin. *J. Clin. Invest.* 91: 1608–1615.
8. Zillikens, D., P. A. Rose, S. D. Balding, Z. Liu, M. Olague-Marchan, L. A. Diaz, and G. J. Giudice. 1997. Tight clustering of extracellular BP180 epitopes recognized by bullous pemphigoid autoantibodies. *J. Invest. Dermatol.* 109: 573–579.
9. Giudice, G. J., D. J. Emery, B. D. Zelickson, G. J. Anhalt, Z. Liu, and L. A. Diaz. 1993. Bullous pemphigoid and herpes gestationis autoantibodies recognize a common non-collagenous site on the BP180 ectodomain. *J. Immunol.* 151: 5742–5750.
10. Amagai, M., K. Tsunoda, H. Suzuki, K. Nishifuji, S. Koyasu, and T. Nishikawa. 2000. Use of autoantigen-knockout mice in developing an active autoimmune disease model for pemphigus. *J. Clin. Invest.* 105: 625–631.
11. Olasz, E. B., J. Roh, C. L. Yee, K. Arita, M. Akiyama, H. Shimizu, J. C. Vogel, and K. B. Yancey. 2007. Human bullous pemphigoid antigen 2 transgenic skin elicits specific IgG in wild-type mice. *J. Invest. Dermatol.* 127: 2807–2817.
12. Nelson, K. C., M. Zhao, P. R. Schroeder, N. Li, R. A. Wetsel, L. A. Diaz, and Z. Liu. 2006. Role of different pathways of the complement cascade in experimental bullous pemphigoid. *J. Clin. Invest.* 116: 2892–2900.
13. Nishifuji, K., M. Amagai, M. Kuwana, T. Iwasaki, and T. Nishikawa. 2000. Detection of antigen-specific B cells in patients with pemphigus vulgaris by enzyme-linked immunospot assay: requirement of T cell collaboration for autoantibody production. *J. Invest. Dermatol.* 114: 88–94.
14. Sitaru, C., S. Mihai, C. Otto, M. T. Chiriac, I. Hausser, B. Dotterweich, H. Saito, C. Rose, A. Ishiko, and D. Zillikens. 2005. Induction of dermal-epidermal separation in mice by passive transfer of antibodies specific to type VII collagen. *J. Clin. Invest.* 115: 870–878.
15. Shimizu, H., J. N. McDonald, A. R. Kennedy, and R. A. Eady. 1989. Demonstration of intra- and extracellular localization of bullous pemphigoid antigen using cryofixation and freeze substitution for postembedding immunoelectron microscopy. *Arch. Dermatol. Res.* 281: 443–448.
16. Shimizu, H., A. Ishida-Yamamoto, and R. A. Eady. 1992. The use of silver-enhanced 1-nm gold probes for light and electron microscopic localization of intra- and extracellular antigens in skin. *J. Histochem. Cytochem.* 40: 883–888.
17. Takae, Y., T. Nishikawa, and M. Amagai. 2009. Pemphigus mouse model as a tool to evaluate various immunosuppressive therapies. *Exp. Dermatol.* 18: 252–260.
18. Shibaki, A., A. Sato, J. C. Vogel, F. Miyagawa, and S. I. Katz. 2004. Induction of GVHD-like skin disease by passively transferred $CD8^+$ T-cell receptor transgenic T cells into keratin 14-ovalbumin transgenic mice. *J. Invest. Dermatol.* 123: 109–115.
19. Bianchi, L., S. Gatti, and G. Nini. 1992. Bullous pemphigoid and severe erythrodermic psoriasis: combined low-dose treatment with cyclosporine and systemic steroids. *J. Am. Acad. Dermatol.* 27: 278.
20. Curley, R. K., and C. A. Holden. 1991. Steroid-resistant bullous pemphigoid treated with cyclosporin A. *Clin. Exp. Dermatol.* 16: 68–69.
21. Thivolet, J., H. Barthelemy, G. Rigot-Muller, and A. Bendelac. 1985. Effects of cyclosporin on bullous pemphigoid and pemphigus. *Lancet* 325: 334–335.
22. Barthélémy, H., J. Thivolet, F. Cambazard, A. Bendelac, G. Mauduit, F. Granier, and A. Frappaz. 1986. [Cyclosporin in the treatment of bullous pemphigoid: preliminary study]. *Ann. Dermatol. Venereol.* 113: 309–313.
23. Chen, R., G. Ning, M. L. Zhao, M. G. Fleming, L. A. Diaz, Z. Werb, and Z. Liu. 2001. Mast cells play a key role in neutrophil recruitment in experimental bullous pemphigoid. *J. Clin. Invest.* 108: 1151–1158.
24. Liu, Z., L. A. Diaz, J. L. Troy, A. F. Taylor, D. J. Emery, J. A. Fairley, and G. J. Giudice. 1993. A passive transfer model of the organ-specific autoimmune disease, bullous pemphigoid, using antibodies generated against the hemidesmosomal antigen, BP180. *J. Clin. Invest.* 92: 2480–2488.
25. Liu, Z., G. J. Giudice, S. J. Swartz, J. A. Fairley, G. O. Till, J. L. Troy, and L. A. Diaz. 1995. The role of complement in experimental bullous pemphigoid. *J. Clin. Invest.* 95: 1539–1544.
26. Jordon, R. E., S. Kawana, and K. A. Fritz. 1985. Immunopathologic mechanisms in pemphigus and bullous pemphigoid. *J. Invest. Dermatol.* 85: 72s–78s.
27. Provost, T. T., and T. B. Tomasi, Jr. 1973. Evidence for complement activation via the alternate pathway in skin diseases, I. Herpes gestationis, systemic lupus erythematosus, and bullous pemphigoid. *J. Clin. Invest.* 52: 1779–1787.
28. Sitaru, C., S. Mihai, and D. Zillikens. 2007. The relevance of the IgG subclass of autoantibodies for blister induction in autoimmune bullous skin diseases. *Arch. Dermatol. Res.* 299: 1–8.
29. Aricha, R., T. Feferman, S. Fuchs, and M. C. Souroujon. 2008. Ex vivo generated regulatory T cells modulate experimental autoimmune myasthenia gravis. *J. Immunol.* 180: 2132–2139.
30. Sheng, J. R., L. Li, B. B. Ganesh, C. Vasu, B. S. Prabhakar, and M. N. Meriggioli. 2006. Suppression of experimental autoimmune myasthenia gravis by granulocyte-macrophage colony-stimulating factor is associated with an expansion of $FoxP3^+$ regulatory T cells. *J. Immunol.* 177: 5296–5306.
31. McGeachy, M. J., L. A. Stephens, and S. M. Anderton. 2005. Natural recovery and protection from autoimmune encephalomyelitis: contribution of $CD4^+CD25^+$ regulatory cells within the central nervous system. *J. Immunol.* 175: 3025–3032.
32. O'Connor, R. A., K. H. Malpass, and S. M. Anderton. 2007. The inflamed central nervous system drives the activation and rapid proliferation of $Foxp3^+$ regulatory T cells. *J. Immunol.* 179: 958–966.
33. Kaul, R., M. Shenoy, E. Goluszko, and P. Christadoss. 1994. Major histocompatibility complex class II gene disruption prevents experimental autoimmune myasthenia gravis. *J. Immunol.* 152: 3152–3157.
34. Zhang, G. X., B. G. Xiao, M. Bakhiet, P. van der Meide, H. Wigzell, H. Link, and T. Olsson. 1996. Both $CD4^+$ and $CD8^+$ T cells are essential to induce experimental autoimmune myasthenia gravis. *J. Exp. Med.* 184: 349–356.
35. Aoki-Ota, M., K. Tsunoda, T. Ota, T. Iwasaki, S. Koyasu, M. Amagai, and T. Nishikawa. 2004. A mouse model of pemphigus vulgaris by adoptive transfer of naive splenocytes from desmoglein 3 knockout mice. *Br. J. Dermatol.* 151: 346–354.
36. Christadoss, P., M. Poussin, and C. Deng. 2000. Animal models of myasthenia gravis. *Clin. Immunol.* 94: 75–87.
37. Mendel, I., N. Kerlero de Rosbo, and A. Ben-Nun. 1995. A myelin oligodendrocyte glycoprotein peptide induces typical chronic experimental autoimmune encephalomyelitis in $H\text{-}2^b$ mice: fine specificity and T cell receptor Vβ expression of encephalitogenic T cells. *Eur. J. Immunol.* 25: 1951–1959.
38. Büdinger, L., L. Borradori, C. Yee, R. Eming, S. Ferencik, H. Grosse-Wilde, H. F. Merk, K. Yancey, and M. Hertl. 1998. Identification and characterization of autoreactive T cell responses to bullous pemphigoid antigen 2 in patients and healthy controls. *J. Clin. Invest.* 102: 2082–2089.
39. Lin, M. S., C. L. Fu, G. J. Giudice, M. Olague-Marchan, A. M. Lazaro, P. Stastny, and L. A. Diaz. 2000. Epitopes targeted by bullous pemphigoid T lymphocytes and autoantibodies map to the same sites on the bullous pemphigoid 180 ectodomain. *J. Invest. Dermatol.* 115: 955–961.
40. Thoma-Uszynski, S., W. Uter, S. Schwietzke, G. Schuler, L. Borradori, and M. Hertl. 2006. Autoreactive T and B cells from bullous pemphigoid (BP) patients recognize epitopes clustered in distinct regions of BP180 and BP230. *J. Immunol.* 176: 2015–2023.
41. Delgado, J. C., D. Turbay, E. J. Yunis, J. J. Yunis, E. D. Morton, K. Bhol, R. Norman, C. A. Alper, R. A. Good, and R. Ahmed. 1996. A common major histocompatibility complex class II allele HLA-DQB1* 0301 is present in clinical variants of pemphigoid. *Proc. Natl. Acad. Sci. USA* 93: 8569–8571.
42. Xu, L., N. Robinson, S. D. Miller, and L. S. Chan. 2001. Characterization of BALB/c mice B lymphocyte autoimmune responses to skin basement membrane component type XVII collagen, the target antigen of autoimmune skin disease bullous pemphigoid. *Immunol. Lett.* 77: 105–111.
43. Sitaru, C., M. T. Chiriac, S. Mihai, J. Büning, A. Gebert, A. Ishiko, and D. Zillikens. 2006. Induction of complement-fixing autoantibodies against type VII collagen results in subepidermal blistering in mice. *J. Immunol.* 177: 3461–3468.
44. Ishikawa, F., M. Yasukawa, B. Lyons, S. Yoshida, T. Miyamoto, G. Yoshimoto, T. Watanabe, K. Akashi, L. D. Shultz, and M. Harada. 2005. Development of functional human blood and immune systems in NOD/SCID/IL2 receptor γ $chain^{null}$ mice. *Blood* 106: 1565–1573.
45. Ito, M., H. Hiramatsu, K. Kobayashi, K. Suzue, M. Kawahata, K. Hioki, Y. Ueyama, Y. Koyanagi, K. Sugamura, K. Tsuji, et al. 2002. NOD/SCID/γ_c^{null} mouse: an excellent recipient mouse model for engraftment of human cells. *Blood* 100: 3175–3182.
46. Kumar, P., H. S. Ban, S. S. Kim, H. Wu, T. Pearson, D. L. Greiner, A. Laouar, J. Yao, V. Haridas, K. Habiro, et al. 2008. T cell-specific siRNA delivery suppresses HIV-1 infection in humanized mice. *Cell* 134: 577–586.
47. Yajima, M., K. Imadome, A. Nakagawa, S. Watanabe, K. Terashima, H. Nakamura, M. Ito, N. Shimizu, M. Honda, N. Yamamoto, and S. Fujiwara. 2008. A new humanized mouse model of Epstein-Barr virus infection that reproduces persistent infection, lymphoproliferative disorder, and cell-mediated and humoral immune responses. *J. Infect. Dis.* 198: 673–682.
48. Watanabe, Y., T. Takahashi, A. Okajima, M. Shiokawa, N. Ishii, I. Katano, R. Ito, M. Ito, M. Minegishi, N. Minegishi, et al. 2009. The analysis of the functions of human B and T cells in humanized NOD/shi-scid/γc^{null} (NOG) mice (hu-HSC NOG mice). *Int. Immunol.* 21: 843–858.

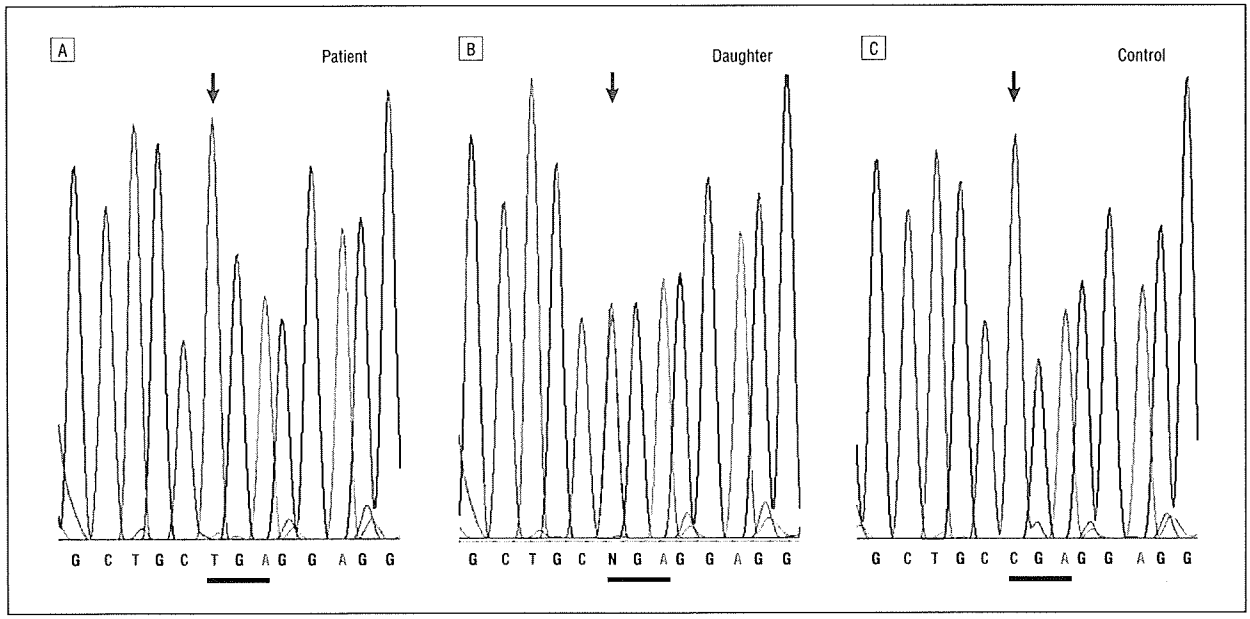

Figure 2. Sequence analysis of the *TAP2* gene. Detection of the mutation from genomic DNA was performed by polymerase chain reaction amplification of *TAP2* exon 3 for the patient (A) (mutant homozygous), a daughter (B) (heterozygous), and a healthy control (C) (native sequence).

previously ulcerated lesions of the right leg (Figure 1D and E), and the limb was amputated. The neoplasia recurred and metastasized, and the patient died.

Blood samples were obtained from the proband and relatives, and lymphocyte subpopulations were analyzed by flow cytometry. The numbers of NK cells, γδ T lymphocytes, and $CD8^+$ αβ T cells as well as the CD4/CD8 ratios were found to be normal and comparable to those found in controls and her relatives. The HLA I expression in the patient's lymphocytes was severely reduced (30 times lower than in healthy controls). The HLA serologic typing in the patient was unsuccessful. We extracted RNA from peripheral blood mononuclear cells; all coding exons of *TAP1* and *TAP2* genes (OMIM 170260 and 170261, respectively) were amplified by reverse transcriptase–PCR, and further sequencing analysis was performed. A previously unreported *TAP2* missense mutation was detected. The patient was homozygous for a C→T transition at nucleotide 628 (*TAP2* exon 3) (**Figure 2**), leading to a premature stop at codon 210 between the fifth and the sixth transmembrane domains of *TAP2*. Her mother and daughters were heterozygous for the mutated allele. In addition, high-resolution molecular HLA typing demonstrated that the patient was homozygous for the haplotype HLA-A*0301, Cw*1701, B*5001, DRB1*0301, DQA*0501/DQB1*0201, and DPB1*0401.

Comment. We report herein an SCC originating in a chronic ulcer of a patient with type I BLS and a novel *TAP2* gene mutation. Abnormal expression of HLA class I has been reported in many human neoplasias,[5] including skin cancer. Our findings suggest that TAP-impaired HLA class I expression could influence the course of SCC originating in chronic ulcers and could be related to escape from cytotoxic T-lymphocyte surveillance during disease progression.

Agustín España, MD
Cecilia González-Santesteban, PhD
Laura Martínez-Martínez, PhD
Ana Bauzá, MD
Oscar de la Calle-Martín, PhD

Correspondence: Dr España, Department of Dermatology, University Clinic of Navarra, School of Medicine, University of Navarra, PO Box 4209, Pamplona, Navarra, Spain (aespana@unav.es).
Financial Disclosure: None reported.

1. de la Salle H, Hanau D, Fricker D, et al. Homozygous human TAP peptide transporter mutation in HLA class I deficiency. *Science.* 1994;265(5169):237-241.
2. Moins-Teisserenc HT, Gadola SD, Cella M, et al. Association of a syndrome resembling Wegener's granulomatosis with low surface expression of HLA class I-molecules. *Lancet.* 1999;354(9190):1598-1603.
3. Peaper DR, Cresswell P. Regulation of MHC class I assembly and peptide binding. *Annu Rev Cell Dev Biol.* 2008;24:343-368.
4. Zimmer J, Andres E, Donato L, Hanau D, Hentges F, de la Salle H. Clinical and immunological aspects of HLA class I deficiency. *QJM.* 2005;98(10):719-727.
5. Garrido F, Ruiz-Cabello F, Cabrera T, et al. Implications for immunosurveillance of altered HLA class I phenotypes in human tumours. *Immunol Today.* 1997;18(2):89-95.

Hereditary Benign Telangiectasia: Two Families With Punctate Telangiectasias Surrounded by Anemic Halos

Hereditary benign telangiectasia (HBT), one of the primary telangiectatic disorders, is characterized by various patterns of widespread cutaneous telangiectasias.[1,2] It is distinguished from hereditary hemorrhagic telangiectasia by the absence of recurrent bleeding and systemic involvement. Herein we describe

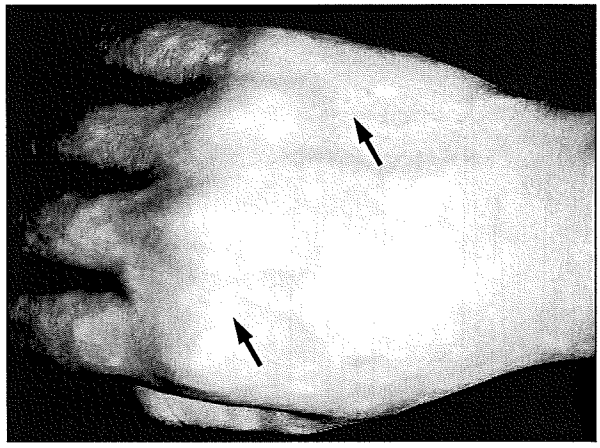

Figure 1. Skin lesions seen on the proband of family 1 with hereditary benign telangiectasia. Multiple punctate telangiectasias surrounded by anemic halos (arrows) are visible on the dorsal surface of the right hand.

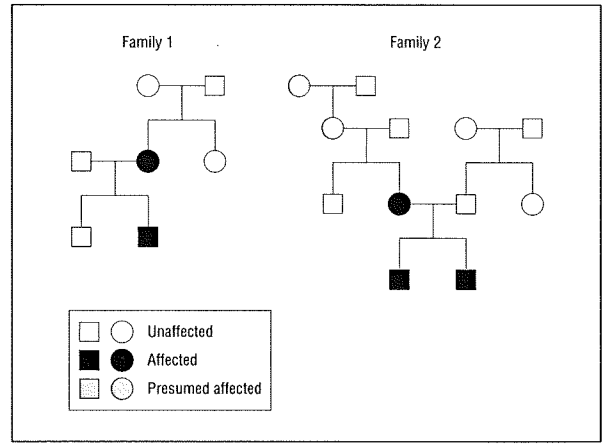

Figure 2. Pedigrees of the 2 families with hereditary benign telangiectasia showing punctate telangiectasias surrounded by anemic halos. Circles indicate female family members; squares, male family members.

2 families with HBT that show unique fine telangiectasias surrounded by anemic halos.

Report of Cases. *Case 1.* A 16-year-old boy was seen for asymptomatic telangiectasias with halos that had appeared several months earlier with no preceding episodes. Physical examination revealed multiple fine telangiectasias surrounded by pale macules as large as 5 mm on the dorsal surfaces of the hands (**Figure 1**), the radial aspects of the forearms and thighs, and on the trunk. The pale macules disappeared during application of mechanical pressure, which indicated that they were anemic halos. He also had numerous fine telangiectasias on the lips and irregularly shaped telangiectatic macules on the chest, right arm, and right thigh. His mother had similar fine telangiectasias surrounded by anemic halos on the right forearm (**Figure 2**). Laboratory data of the proband showed no abnormalities in blood cell count, liver function, renal function, or blood coagulation time. Skin specimens obtained from a telangiectasia with an anemic halo on the dorsal surface of the proband's hand demonstrated no specific changes. All of the telangiectatic lesions persisted for more than 5 years.

Case 2. A 14-year-old boy was referred for evaluation of asymptomatic fine telangiectasias surrounded by halos that had been noticed several weeks earlier without any preceding episodes. Multiple punctate telangiectasias surrounded by anemic halos were seen on the dorsal surfaces of the hands and on the radial aspects of the forearms. He had some irregularly shaped telangiectatic macules on the face, trunk, and extremities.

His mother had macular telangiectasias on her back and face, and his 11-year-old brother had similar lesions on his left hand and upper extremities (Figure 2). None of the family members had remarkable medical histories or hemorrhagic episodes. His maternal grandmother and great-grandmother seemed to have some reddish macular lesions, but the details were unclear (Figure 2).

No specific abnormalities were detected in laboratory examinations of the proband. Histologic and ultrastructural examinations of the biopsy specimens from the proband demonstrated no specific changes. To date, the cutaneous lesions of the proband remain unchanged for over 5 years.

Comment. Initially described in 1971,[2] HBT is probably an autosomal dominant disorder.[1] Various patterns of telangiectatic lesions, including plaquelike, radiating, arborizing, reticulated, mottled, spiderlike, and punctate, have been described in HBT.[1,2] Punctate telangiectasias surrounded by anemic halos have rarely been reported.[3] The mechanism whereby the anemic halo develops remains unclear. In eruptive pseudoangiomatosis, a rare skin disorder characterized by acute angiomalike papules or macules, the surrounding halo might be due to vasoconstriction around the vasodilatation of the papular angiomatous lesions.[4] In nevus anemicus, the anemic macule is thought to be caused by increased local vascular reactivity to catecholamines.[5] The findings from the families described herein indicate that punctate telangiectasias surrounded by anemic halos should be recognized as unique and characteristic features of HBT.

Hideyuki Ujiie, MD
Kazuo Kodama, MD, PhD
Masashi Akiyama, MD, PhD
Hiroshi Shimizu, MD, PhD

Correspondence: Dr Ujiie, Department of Dermatology, Hokkaido University Graduate School of Medicine, N15 W7, Kita-ku, Sapporo 060-8638, Japan (h-ujiie@med.hokudai.ac.jp).
Financial Disclosure: None reported.
Additional Contributions: Kokichi Hamasaka, MD, provided helpful information on the cases.

1. Brancati F, Valente EM, Tadini G, et al. Autosomal dominant hereditary benign telangiectasia maps to the CMC1 locus for capillary malformation on chromosome 5q14. *J Med Genet.* 2003;40(11):849-853.
2. Ryan TJ, Wells RS. Hereditary benign telangiectasia. *Trans St Johns Hosp Dermatol Soc.* 1971;57(1):148-156.
3. Puppin D Jr, Rybojad M, Morel P. Hereditary benign telangiectasia: two case reports. *J Dermatol.* 1992;19(6):384-386.
4. Neri I, Patrizi A, Guerrini V, Ricci G, Cevenini R. Eruptive pseudoangiomatosis. *Br J Dermatol.* 2000;143(2):435-438.
5. Greaves MW, Birkett D, Johnson C. Nevus anemicus: a unique catecholamine-dependent nevus. *Arch Dermatol.* 1970;102(2):172-176.

Successful Treatment of Nail Lichen Planus with Topical Tacrolimus

Hideyuki Ujiie, Akihiko Shibaki, Masashi Akiyama and Hiroshi Shimizu
Department of Dermatology, Hokkaido University Graduate School of Medicine, North 15 West 7, Kita-ku, Sapporo 060-8638, Japan. E-mail: h-ujiie@med.hokudai.ac.jp
Accepted November 4, 2009.

Sir,

Nail lichen planus (NLP) is characterized by thinning, longitudinal ridging and distal splitting of the nail plate (1, 2). Although mild NLP is usually asymptomatic, deformation of the fingernails is cosmetically distressing. Failure to treat NLP results in nail loss or permanent nail dystrophy in some cases. Therefore the condition should be treated effectively in its early stage. NLP is usually resistant to topical corticosteroid therapy, but successful treatment has been reported with intralesional or systemic administration of corticosteroids (2–4). However, some patients are unable to tolerate the side-effects of systemic corticosteroids.

Topical tacrolimus has been reported as a safe, effective therapy for cutaneous (5, 6), oral (7–9) and vulvar lichen planus (LP) (9–11), even in patients whose lesions have shown recalcitrance to other treatments (7, 10). However, topical tacrolimus treatment for NLP has never been reported. We report here five cases of NLP treated successfully with tacrolimus ointment.

CASE REPORTS

Five Japanese patients with NLP were treated with 0.1% tacrolimus ointment. The mean age of the five patients (4 males and 1 female) was 40.2 years (age range 11–58 years). All of the patients were diagnosed with NLP on the basis of clinical history, typical clinical appearance and histopathological features. No patient had any symptoms suggesting lupus erythematosus or photosensitivity. There was no history of nail matrix trauma, or drug intake that could cause lichenoid drug eruption. All of these cases demonstrated multiple nail lesions on the fingers and/or toes. In one patient, the disease affected all 20 nails. All the fingernails were affected in three other patients, including two cases that presented with additional nail lesions on both big toes. The most common clinical signs were thinning of nails and onycholysis, which were observed in all of the patients. Longitudinal ridging and onychorrhexis were present in four cases. The NLP was not associated with any objective symptom, such as burning, itching or pain, in any of the cases. A 58-year-old patient had concomitant localized reticular oral LP, although no patient had cutaneous, otic or genital lesions at any time during the follow-up. An 11-year-old patient had mild atopic dermatitis; the four adult patients had no other dermatological conditions. The clinical diagnosis was confirmed by histopathological examination in all cases. Biopsy specimens taken from the affected nail matrix demonstrated band-like lymphocyte infiltration in the nail matrix and the nail bed dermis, as well as hyperkeratosis, acanthosis and hypergranulosis of the epidermis, which are histopathological features typically observed in NLP.

The mean duration of the disease prior to the topical tacrolimus treatment was 24 months (range 4–84 months). We followed up all the patients for at least 15 months (mean 39.0 months; range 15–71 months). Four of the patients had been treated with topical corticosteroids, with no or slight improvement, before the tacrolimus therapy. In all the cases, 0.1% topical tacrolimus (Protopic ointment 0.1%, Astellas Pharma Inc., Tokyo, Japan) was administered twice a day on one side of the nail plates and periungual regions of the fingers and/or toes, and a topical corticosteroid (from the classification "very strong" or "strongest") was simultaneously started on the other side for a comparison of relative efficacy. In all cases, the affected nails treated with topical tacrolimus began to improve within 6 months after the initiation of treatment (mean 2.8 months; range 1–6 months), whereas no obvious changes, or only slight improvement, were observed in the nails treated with topical corticosteroids, suggesting that tacrolimus ointment had higher therapeutic efficacy than topical corticosteroids (Fig. 1). All the lesions were then treated uniformly with topical tacrolimus. All of the patients showed marked improvement (Fig. 2). Mild onycholysis and splitting of the nails remained in some of the patients. Reticular oral LP observed in a 58-year-old patient remained after his NLP lesions had improved. Two patients who discontinued topical tacrolimus application showed no exacerbation of their lesions at 16 and 36 months of follow-up, respectively. Two other patients continue to use topical tacrolimus once or twice daily as a supportive treatment, which keeps their lesions stable. The remaining patient stopped visiting our clinic after remission. No adverse effects were noted in any of the cases.

DISCUSSION

Topical corticosteroid therapy is commonly considered as a first-line treatment for NLP, although it is usually ineffective. Oral prednisone and intramuscular triamcinolone acetonide have been reported as effective against NLP (2–4), but prolonged or repeated use of

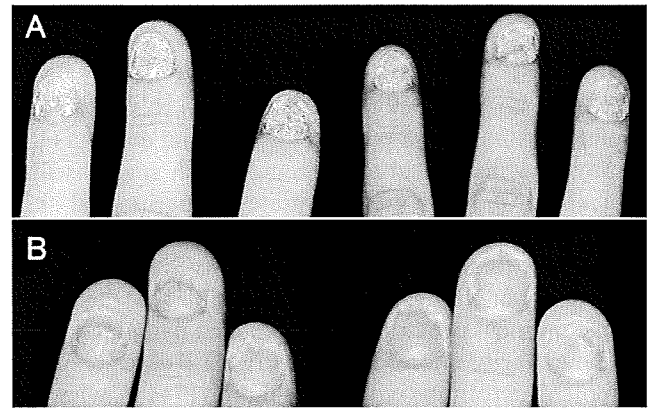

Fig. 1. (A) Nail lichen planus in an 11-year-old male patient before treatment. The fingernails show very severe thinning. The right-hand fingernails were treated with topical tacrolimus and the left-hand ones with diflucortolone valerate ointment twice daily (comparative application). (B) The same patient after 5 months of comparative application. Significant clinical improvement of the right-hand fingernails (*right*) was noted compared with the left-hand ones (*left*).

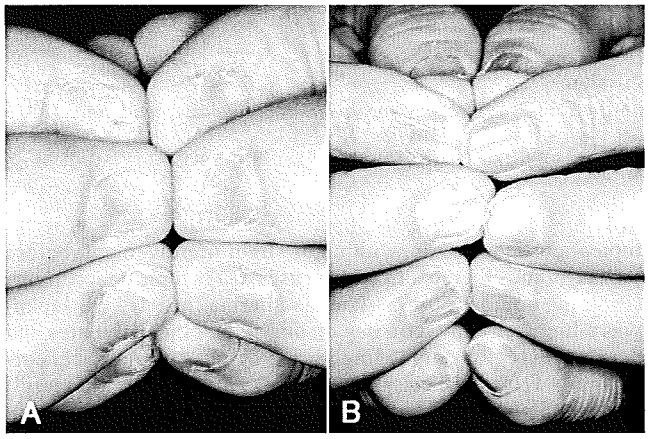

Fig. 2. (A) Nail lichen planus in a 58-year-old male patient. The fingernails show severe distal thinning and onycholysis before treatment. (B) Significant improvement after 18 months of topical tacrolimus treatment.

systemic corticosteroids may cause considerable side-effects.

Tacrolimus is a macrolide immune modulator that produces strong immunosuppression by inhibiting T-cell activation. It interacts with a cyclophilin-like cytoplasmic protein, FK506 binding protein, and this complex interferes with the phosphatase activity of calcineurin, resulting in the inhibition of proinflammatory cytokine genes transcription. Because activated T cells are likely to play a central role in the pathogenesis of LP (1, 12, 13), topical tacrolimus has been tried for the treatment of LP. Previous studies have reported that topical tacrolimus is effective for 88–100% of cases of oral LP (7–9) and 94% of cases of vulvar LP (10). Based on these data, we speculated that topical tacrolimus could also be effective against NLP. In this study, all five cases with NLP responded fairly well to topical tacrolimus, even though 4 had intractable lesions that had shown resistance to topical corticosteroids. Comparative study of the efficacy of topical tacrolimus and topical corticosteroids revealed that topical tacrolimus was more effective than topical corticosteroids in all of the cases.

Recent studies demonstrated that nail dystrophy associated with chronic paronychia (14) and eczema (15) improved with topical tacrolimus, which suggests that topical tacrolimus could penetrate the periungual skin enough to improve the nail dystrophy. In addition, the remarkable thinning of the nails and onychorrhexis seen in most of our NLP cases make it possible that the tacrolimus ointment penetrated the damaged nail plates.

The majority of oral LP and vulvar LP cases respond to topical tacrolimus within one month (7–11), whereas the present NLP patients required several months to start to regress (mean 2.8 months).

At present, two out of the five patients have been continuing once- or twice-daily application for 35 and 63 months, respectively, to keep their lesions under control. Two other patients have been stable without topical tacrolimus for more than one year. However, we should be aware of the possibility that NLP can recur, because previous reports have mentioned that oral or vulvar LP lesions usually returned after withdrawal of topical tacrolimus (7, 10). Further analysis with longer follow-up is required to confirm the long-term prognosis of NLP after the cessation of topical tacrolimus therapy.

The authors declare no conflict of interest.

REFERENCES

1. Boyd AS, Neldner KH. Lichen planus. J Am Acad Dermatol 1991; 25: 593–619.
2. Tosti A, Peluso AM, Fanti PA, Piraccini BM. Nail lichen planus: clinical and pathologic study of twenty-four patients. J Am Acad Dermatol 1993; 28: 724–730.
3. Evans AV, Roest MA, Fletcher CL, Lister R, Hay RJ. Isolated lichen planus of the toe nails treated with oral prednisolone. Clin Exp Dermatol 2001; 26: 412–414.
4. Tosti A, Piraccini BM, Cambiaghi S, Jorizzo M. Nail lichen planus in children: clinical features, response to treatment, and long-term follow-up. Arch Dermatol 2001; 137: 1027–1032.
5. Al-Khenaizan S, Al Mubarak L. Ulcerative lichen planus of the sole: excellent response to topical tacrolimus. Int J Dermatol 2008; 47: 626–628.
6. Fortina AB, Giulioni E, Tonin E. Topical tacrolimus in the treatment of lichen planus in a child. Pediatr Dermatol 2008; 25: 570–571.
7. Byrd JA, Davis MD, Bruce AJ, Drage LA, Rogers RS, 3rd. Response of oral lichen planus to topical tacrolimus in 37 patients. Arch Dermatol 2004; 140: 1508–1512.
8. Olivier V, Lacour JP, Mousnier A, Garraffo R, Monteil RA, Ortonne JP. Treatment of chronic erosive oral lichen planus with low concentrations of topical tacrolimus: an open prospective study. Arch Dermatol 2002; 138: 1335–1338.
9. Vente C, Reich K, Rupprecht R, Neumann C. Erosive mucosal lichen planus: response to topical treatment with tacrolimus. Br J Dermatol 1999; 140: 338–342.
10. Byrd JA, Davis MD, Rogers RS, 3rd. Recalcitrant symptomatic vulvar lichen planus: response to topical tacrolimus. Arch Dermatol 2004; 140: 715–720.
11. Kirtschig G, Van Der Meulen AJ, Ion Lipan JW, Stoof TJ. Successful treatment of erosive vulvovaginal lichen planus with topical tacrolimus. Br J Dermatol 2002; 147: 625–626.
12. Shiohara T, Moriya N, Nagashima M. The lichenoid tissue reaction. A new concept of pathogenesis. Int J Dermatol 1988; 27: 365–374.
13. Shiohara T, Nickoloff BJ, Moriya N, Gotoh C, Nagashima M. In vivo effects of interferon-gamma and anti-interferon-gamma antibody on the experimentally induced lichenoid tissue reaction. Br J Dermatol 1988; 119: 199–206.
14. Rigopoulos D, Gregoriou S, Belyayeva E, Larios G, Kontochristopoulos G, Katsambas A. Efficacy and safety of tacrolimus ointment 0.1% vs. betamethasone 17-valerate 0.1% in the treatment of chronic paronychia: an unblinded randomized study. Br J Dermatol 2009; 160: 858–860.
15. Lee DY, Kim WS, Lee KJ, Kim JA, Park JH, Cho HJ, et al. Tacrolimus ointment in onychodystrophy associated with eczema. J Eur Acad Dermatol Venereol 2007; 21: 1137–1138.

Journal of Dermatological Science 57 (2010) 102–107

Contents lists available at ScienceDirect

Journal of Dermatological Science

journal homepage: www.elsevier.com/jds

Epidermal triglyceride levels are correlated with severity of ichthyosis in Dorfman–Chanarin syndrome

Mayumi Ujihara [a], Kimiko Nakajima [a], Mayuko Yamamoto [a], Mika Teraishi [a], Yoshikazu Uchida [b], Masashi Akiyama [c], Hiroshi Shimizu [c], Shigetoshi Sano [a,*]

[a] Department of Dermatology, Kochi Medical School, Kochi University, Oko-cho, Nankoku, Japan
[b] Department of Dermatology, School of Medicine, University of California San Francisco, CA, USA
[c] Department of Dermatology, Hokkaido University Graduate School of Medicine, Sapporo, Japan

ARTICLE INFO

Article history:
Received 17 July 2009
Received in revised form 28 October 2009
Accepted 29 October 2009

Keywords:
Dorfman–Chanarin syndrome
Neutral lipid storage disease with ichthyosis
Triglycerides
CGI-58

ABSTRACT

Background: Dorfman–Chanarin syndrome (DCS), also referred to as neutral lipid storage disease with ichthyosis, is a rare autosomal recessive form of nonbullous congenital ichthyosiform erythroderma, characterized by the presence of intracellular lipid droplets in multiorgans. DCS patients often have mutations in CGI-58, which is an activator of adipose triglyceride lipase (ATGL), leading to accumulation of triglycerides (TG).
Objective: To study whether a patient with DCS demonstrates TG accumulation in the epidermis and to analyze whether TG levels are correlated with skin disease activity.
Methods: Skin specimen from a 62-year-old man with DCS was stained with oil red O, and analyzed on electromicrographs. Sequencing analysis of *CGI-58* was performed using the patient's blood cells. The scales from the lesion were subject to lipid analysis by high-performance thin-layer chromatography (HPTLC).
Results: The patient demonstrated ichthyoform erythroderma with a distinct seasonal fluctuation: his skin lesions were aggravated in summer but resolved during winter. Epidermis of the lesion showed intracellular lipid droplets. Sequencing analysis revealed a novel missense mutation in the exon 3 of *CGI-58* gene. Lipid analysis of the scales from his lesions, compared with those from normal human control, revealed increased levels of triglycerides (TG) but, in turn, decreased levels of free fatty acids, suggesting dysfunction of adipose TG lipase. Notably, the TG levels in the scales from the patient were positively correlated with the severity of ichthyosis.
Conclusion: These results suggest that TG accumulation by epidermal keratinocytes directly contributes to ichthyosiform phenotype of DCS.

1. Introduction

Dorfman–Chanarin syndrome (DCS, MIM275630), also referred to as neutral lipid storage disease with ichthyosis (NLSDI), is a rare autosomal recessive disorder, in which an excess of triacylglycerols (TG) accumulates in various cells [1–3]. DCS is characterized by nonbullous congenital ichthyosiform erythroderma associated with the presence of cytoplasmic neutral lipid droplets in keratinocytes, as well as a variety of cells in the body including peripheral leukocytes (Jordans' anomaly) [4] and liver cells [5]. Therefore, extracutaneous manifestations of DCS include hepatomegaly (fatty liver), myopathy, cataract, sensoryneural deafness and other neurological symptoms. While cutaneous manifestation of DCS represented nonbullous congenital ichthyosiform erythroderma of mild to moderate severity, the clinical heterogeneity is present. For example, they included nonspecific ichthyosiform dermatosis with alopecia [5], sparing of the face [6], or even no erythematous change [7]. In addition, a case with DCS exhibited ichthyotic erythematous plaques, which frequently migrated as a clinical feature resembling erythrokeratoderma variabilis [8].

Mutations in *CGI-58* gene, which is also called *ABHD5* and encodes a member of α/β-hydrolase family of proteins, have been identified as a cause of DCS [9]. CGI-58 is an activator of adipose triglyceride lipase (ATGL) contributing to TG lipolysis [10,11], which depends on its association with perilipin [12]. CGI-58 mutations, therefore, abrogated lipolysis and induced a systemic accumulation of lipids droplets. *CGI-58* gene is located on 3p21, encoding seven exons, and expressed in many tissues including

* Corresponding author. Tel.: +81 88880 2363; fax: +81 88880 2364.
E-mail address: sano.derma@kochi-u.ac.jp (S. Sano).

0923-1811/$36.00
doi:10.1016/j.jdermsci.2009.10.016

skin [9,13]. In patients with DCS, *CGI-58* mutations were associated with defective formation of lamellar granules [14]. Lipid micro-inclusions in lamellar granules formed a non-lamellar phase within the stratum corneum interstices, contributing to permeability barrier dysfunction characterized by ichthyosis in DCS [15]. To date, 16 mutations of *CGI-58* gene have been reported [16], and each of mutations affected the structure of CGI-58, leading to dysfunction of the downstream lipase ATGL. The mutations found in DCS include missense mutations, nonsense mutations, splice site mutations, a deletion or insertion in exons causing a frameshift and premature termination of translation [9,14]. For instance, forced expression of mutant *CGI-58* gene into an adipocyte cell line resulted in its inability to interact with perilipin, leading to mistargeting of CGI-58 to the lipid droplets [12]. Further, expression of functional CGI-58 in DCS fibroblasts restores lipolysis and reversed the abnormal TG accumulation [10].

Mutations in the gene encoding ATGL (*PNPLA2*) have been identified as the cause of neutral lipid storage disease with myopathy (NLSDM) [17]. NLSDM patients and ATGL-deficient mice exhibited DCS-like features associated with TG accumulation in multiple tissues including adipose tissue, muscle, heart and other organs, however, devoid of ichthyosis [18,17].

Therefore, the mutations in *CGI-58* gene result in development of ichthyosis in addition to abnormalities shared with NLSDM. This notion indicated that CGI-58 possessed an additional function required for lipid metabolism in the epidermis [17]. Previous studies demonstrated that the ultrastructure of DCS included abnormal lipid micro-inclusions within lamellar bodies and resulting lamellar/non-lamellar phase separation or clefts in the intercellular spaces of cornified layer [3,14,15]. Very recent study revealed that CGI-58 expression was increased during differentiation and localized in lamellar granules of keratinocytes and likely to be involved in barrier formation [13]. Given that TG is the content of lipid deposition in DCS, unsolved question is that the ultrastructural aberrancy in the epidermis is similar to other inherited, lipid storage diseases associated with ichthyosis, such as Refsum disease, Sjögren–Larsson syndrome [15]. Thus, no direct evidence has been shown regarding the link of TG deposition in the epidermis and ichthyosiform phenotype found in DCS.

In the present study, we demonstrate a DCS patient with a novel mutation of *CGI-58* gene in one allele, showing an abrupt, seasonal variation of ichthyosiform lesions. Biochemical study of his scales revealed the increased levels of TG, which was positively correlated with severity of ichthyosis.

2. Materials and methods

2.1. Patient

This study was approved by the Institute Ethical Review Board of the Kochi Medical School, Kochi University, and performed according to the Declaration of Helsinki Principles. Skin samples and scales were provided from a patient with DCS (see Section 3 for further details) and healthy donors with sunburn as controls.

2.2. Electron microscopic examination

The skin biopsy specimens were fixed with 2% glutaraldehyde in 0.1 M sodium cacodylate (pH 7.3) for 2 h at room temperature. The skin samples were post-fixed for 1 h at room temperature with 2% osmium tetroxide in 0.1 M cacodylate buffer. The samples were then dehydrated in a graded series of ethanol. Following dehydration, the samples were transferred to propylene oxide and embedded in Epon 812 (TAAB Laboratories Equipment, Berkshire, England). They were observed with a Hitachi H-7100 electron microscope (Hitachi High-Technologies, Tokyo, Japan).

2.3. Determination of TEWL and water holding capability

To assess basal permeability barrier function, we used a Tewameter (TEWAMETER TM300, Courage and Khazaka, Cologne, Germany) over six separate sites. Water holding capability was determined using a corneometer (CORNEOMETER CM825, Courage and Khazaka) over six separate sites.

2.4. Mutation analysis

The method for mutation detection of *CGI-58* gene was performed as previously reported [9]. Briefly, genomic DNA isolated from peripheral blood was subject to PCR amplification, followed by direct automated sequencing. Oligonucleotide primers used for amplification of all exons 1–7 of *CGI-58* gene and detailed PCR conditions were described elsewhere [14,9].

2.5. Lipid analysis of scales

Total lipids were extracted from scales as described previously [19]. Scales from sunburn in a healthy individual were used as control for this assay, since we confirmed that its lipid content did not significantly differ from that previously reported from non-sunburn scales in normal donors. The individual lipid species were separated by high-performance thin-layer chromatography (HPTLC), followed by quantification by scanning densitometry as described previously with the following solvent systems: (1) benzene–n-hexane (1:1) to 8.5 cm; and n-hexane–diethyl ether–acetic acid (70:30:1, v/v/v) to 5 cm. Lipids were visualized after treatment with cupric acetate–phosphoric acid, and heating to 160 °C for 15 min. The quantity of each lipid was determined by spectrodensitometry, as previously described [19].

3. Results

3.1. Case presentation

A 62-year-old Japanese man visited our hospital in October 2006 complaining of slightly pruritic, dry skin with scaling. From early childhood the patient had been suffering from scaly skin lesions over the entire body, which were characterized by a seasonal variation with a marked aggravation in summer. He was the first and an only child from non-consanguineous parents. There was no family history of congenital ichthyosis or abnormal lipid diseases. The patient was mildly obese with a BMI 26.5 (height: 157 cm, weight: 65 kg). His skin was dry and mildly erythrodermic with fine scales, surrounding normal-looking skin with irregular patterns on the trunk, lateral side of upper arms, the right scapular region, bilateral breasts, and buttocks (Fig. 1a and b). The skin of the dorsa of the hands was shiny with prominent creases and lamellar scaling was in lower legs (Fig. 1c). There were spiny keratoses on his palms, but the nails, teeth and hair appeared normal.

Transepidermal water loss (TEWL) and skin hydration were assessed in the involved skin and normal-looking, uninvolved skin of the upper arm. TEWL of the ichthyosiform lesion (18.0 g h^{-1} m^{-2}) was within the normal range (0–10, very good; 10–15, good; 15–20, fair; 25–30, poor; more than 30, very poor) but slightly higher than uninvolved skin (14.5 g h^{-1} m^{-2}). On the other hand, the water retention capability was markedly impaired in the lesion (6.7, normal >60) compared with the uninvolved skin (63.8). These results indicated that the ichthyosiform lesions of this patient showed an intact permeability barrier but a markedly decreased hydration, which was contrast to a previous study showing abnormal barrier function [15].

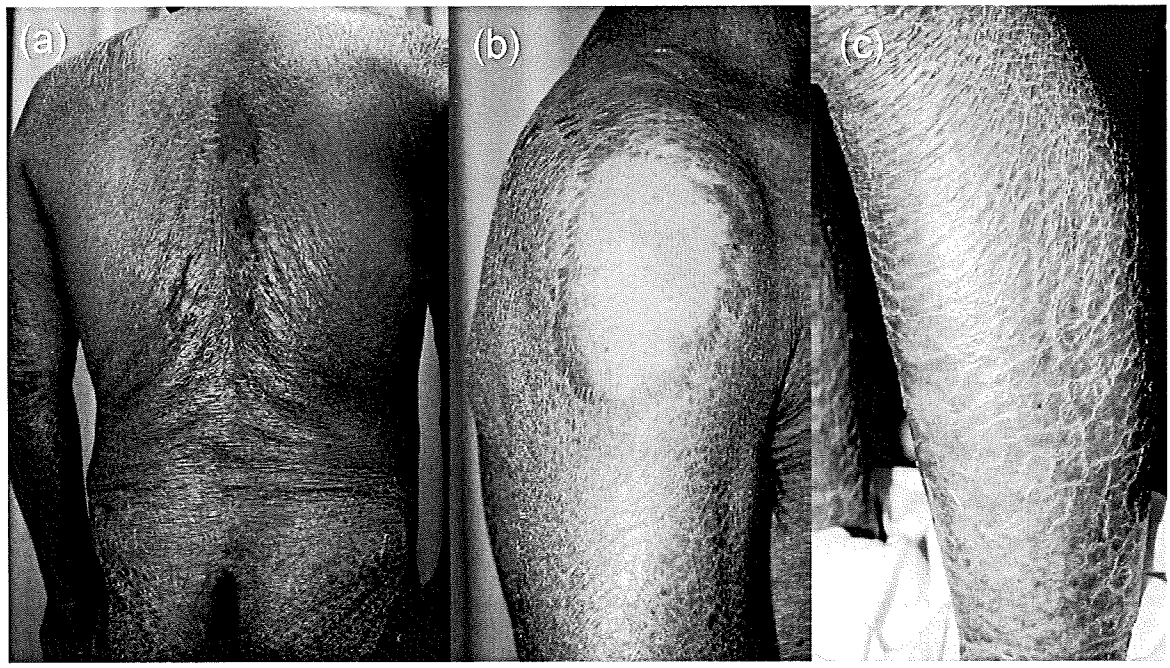

Fig. 1. Clinical appearance. (a) Scaly ichthyosiform erythroderma. (b) Sharply demarcated site of uninvolved skin on the lateral aspect of the upper arm. (c) Large, membranous scales on the legs.

Laboratory investigation revealed abnormalities of hepatic enzymes including aspartate aminotransferase 85 IU L^{-1} (normal range: 10–35), alanine aminotransferase 79 IU L^{-1} (5–40), γ-glutamyltransferase 497 IU L^{-1} (5–70), and alkaline phosphatase 366 IU L^{-1} (100–344). The computed tomography and ultrasonic examination demonstrated hepatic hypertrophy and fatty liver. Steroid sulfatase activity in the peripheral blood sample was normal. Although white blood cell count was normal, there were distinct intracytoplasmic vacuoles in polynuclear leukocytes (Fig. 2c) and monocytes (Fig. 2d), which were presumed to be Jordan's anomaly [4]. No evidence of muscle weakness or neurological abnormality was obtained.

3.2. Histologic features and lipid droplets in the epidermis

Skin biopsy specimen from the right thigh revealed hyperkeratosis and mild acanthosis but the granular layer was normal (Fig. 2a). There were mild mononuclear cell infiltrates around blood vessels in the dermis. Groups and strands of fat cells were found embedded among the proliferating collagen bundles of the

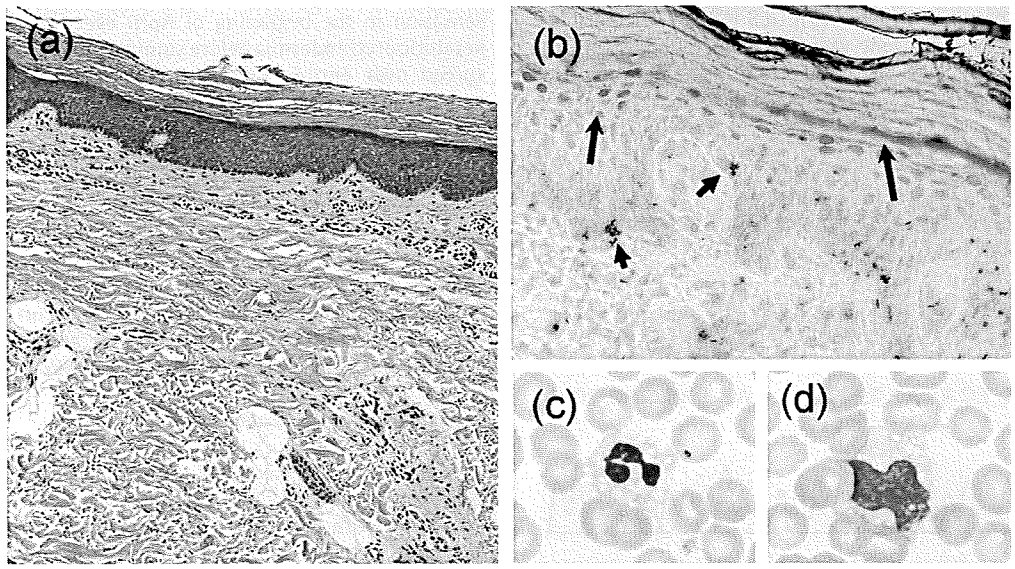

Fig. 2. Histologic appearance and lipid deposition in epidermis and white blood cells. (a) H&E staining of formalin-fixed, paraffin-embedded lesional skin section from the patient's left thigh. Hyperkeratosis, acanthosis and mild perivascular infiltrates are noted (40×). (b) Oil red O staining of frozen section (200×). The cornified and granular layers are strongly stained with oil red O (arrows), which also stained cells of basal layer in punctate (arrowheads). Intracytoplasmic vacuoles within peripheral blood neutrophils (c, 1000×) and monocytes (d, 1000×) represent Jordan's anomaly.

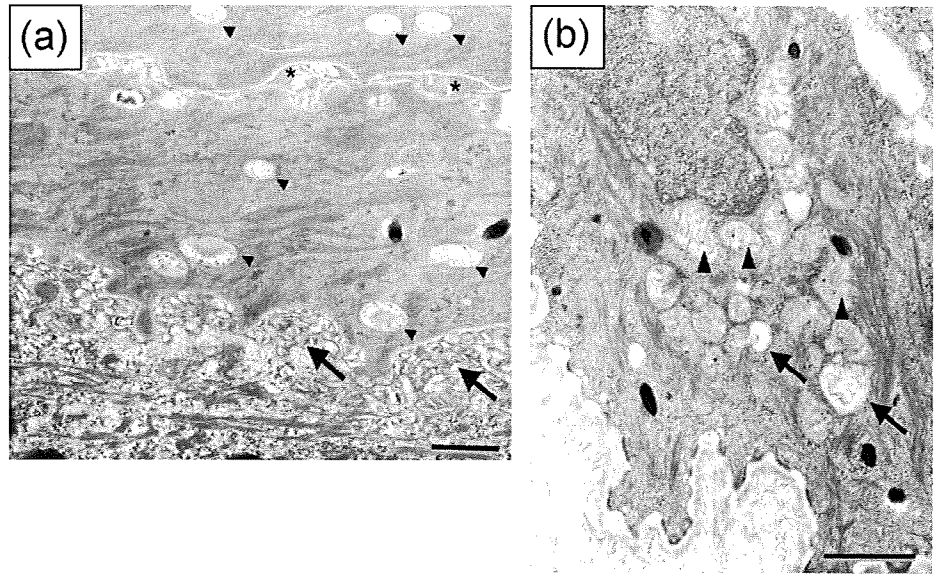

Fig. 3. Electron micrographs after osmium tetroxide post-fixation and Epon embedding. (a) Electron-lucent vacuoles are present within corneocytes (arrowheads). There are amorphous materials in the intracellular spaces (asterisks). Abnormal lamellar granules are aggregated in the stratum granulosum/stratum corneum interface (arrows). Scale bar, 0.5 μm. (b) Giant mitochondria (arrowheads) and lucent vacuoles (arrows) are seen in the cytoplasm of basal cells. Scale bar, 1 μm.

dermis (Fig. 2a). Staining with oil red O demonstrated lipid droplets within keratinocytes in the stratum granulosum, the stratum corneum (Fig. 2b, arrows) and the basal layer (Fig. 2b, arrowheads). Taken together, we diagnosed him as DCS.

3.3. Ultrastructural findings

Electron microscopic examination of the lesional skin of the patient revealed a number of electron-lucent vacuoles, presumably lipid droplets, within the cytoplasm of corneocytes and deposits of amorphous materials in the intercellular spaces (Fig. 3a). Accumulation of abnormal lamellar granules lacking the normal lamellar content was also seen in the stratum granulosum/stratum corneum interface (arrows in Fig. 3a). These features were consistent with previous studies with DCS [14,15]. Furthermore, giant mitochondria and lucent vacuoles were found within the basal keratinocytes (Fig. 3b), suggesting an abnormal lipid metabolism of keratinocytes as previously described [20].

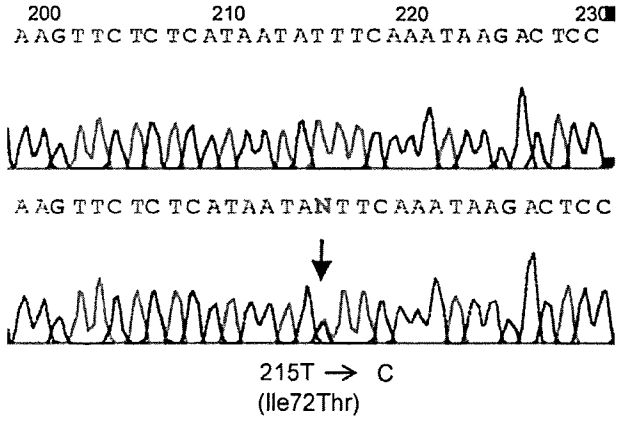

Fig. 4. Sequencing analysis of *CGI-58* gene. A novel heterozygous 215T>C transition in the exon 3, that substitutes isoleucine for threonine at position 72 (I72T).

3.4. Mutation in CGI-58 gene

Mutation analysis of *CGI-58* gene of the patient's blood revealed a heterozygous point mutation (215T>C) in the exon 3 (Fig. 4). This novel mutation substituted isoleucine for threonine at position 72 (Ile72Thr), indicating a missense mutation. However, further analysis of another allele failed to detect any other pathogenic mutation within the all seven exons and exon–intron borders of this gene (data not shown).

3.5. Seasonal variation of disease activity

Notably, his skin lesions were aggravated in summer. As shown in Fig. 5, the ichthyosiform lesions recurred with some irritant sensation in the beginning of April every year, and developed keratotic erythrodermia before summer. The ichthyosiform lesions spread over entire body, but several areas were spared, for example, around nipples. This manifestation was very similar to a previous report, in which a patient with DCS showed erythematous migratory patches resembling erythrokeratoderma variabilis [8]. With lowering the air temperature in autumn, the ichthyosiform plaques were remitted, and mostly, if any, disappeared by mid-winter. Interestingly, his skin lesions showed some resolution when he stayed away from hot temperature even in the mid-summer, but were immediately aggregated when stayed outside. This suggested that the development of the ichthyosiform change was dependent on environmental temperature. Such feature was also similar to the aforementioned DCS patient [8].

3.6. Lipid analysis of scales

Scales were collected from the involved sites of the patient at aggravation and remission stages. Scales from a non-ichthyotic individual with sunburn dermatitis were used as a control. Although there was no difference in the quantity of cholesterol between the patient and control, triglycerides (TG) were increased by two- and threefold over control in the scales at remission and aggravation stage, respectively (Fig. 6). Thus, TG levels in scales were correlated with the severity of ichthyotic condition. In

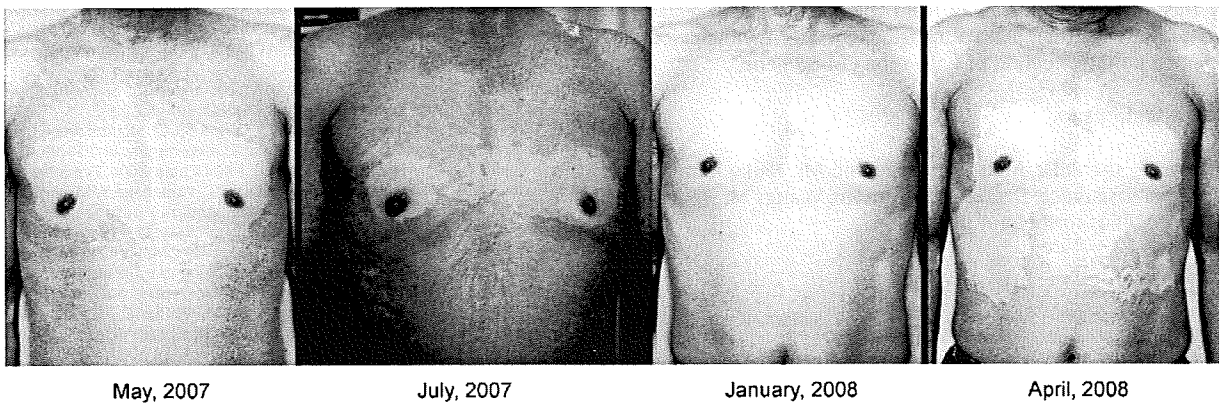

Fig. 5. Distinct seasonal variation of ichthyosis. Ichthyosiform lesions were aggravated from spring and formed erythroderma throughout hot season, but ameliorated in winter.

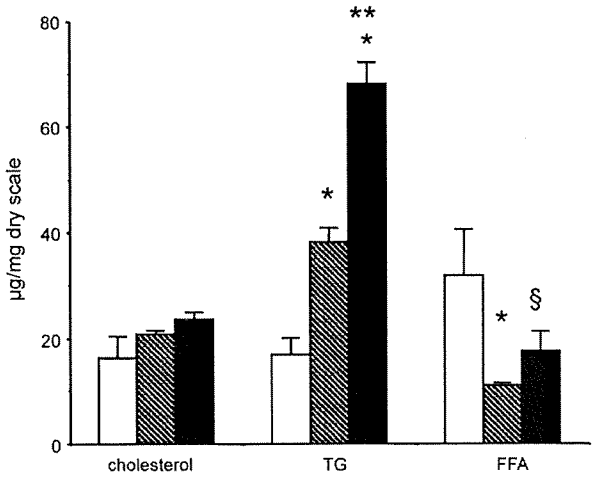

Fig. 6. Lipid analysis of scales taken from sunburn lesion as controls (white bar), patient's lesions at aggravation and remission stages (black, shaded bars, respectively), showing positive correlation of increased TG levels with disease severity. FFA levels are invariably decreased in patient's scales. Mean ± s.d. μg/mg dry scale. $^{*}p < 0.01$ vs. control. $^{**}p < 0.01$ vs. remission stage. $^{\S}p < 0.02$ vs. control.

contrast, free fatty acids were invariably decreased in the patient's scales compared with control. These results were relevant, since DCS is characterized by dysfunction of CGI-58, an activator of ATGL, which hydrolyzes TG to release FFA.

4. Discussion

Dorfman–Chanarin syndrome (DCS) is defined as a neutral lipid storage disorder with ichthyosis (NLSDI), which is attributed to mutations in CGI-58. Since CGI-58 is an activator of adipose triglyceride lipase (ATGL), patients with DCS demonstrated systemic storage of triglycerides as found in patients with mutations in ATGL, which were designated a neutral lipid storage disorder with myopathy (NLSDM). However, NLSDM patients and ATGL-deficient mice did not develop ichthyosis [17,18]. It was, therefore, hypothesized that CGI-58 could have an additional metabolic function required for normal skin physiology [17]. This hypothesis was supported by the fact that the lipid accumulation in the epidermis was higher in DCS than in NLSDM [17].

Sequencing analysis of the *CGI-58* gene using the patient's blood cells revealed a novel missense mutation in nucleotide position 215 (T>C) within the exon 3. As far as we examined, however, no mutation of this gene was found in another allele. Moreover, RT-PCR using primer sets specific for some exons including the exon 3 demonstrated no mRNA alteration in quantity and size compared to healthy controls (data not shown). Therefore, it was unlikely that truncation or instability of this gene occurred in our patient. His family history suggested that the inheritance was recessive, although there was no DCS patient among his relatives. It remained unsolved whether he had another undefined mutation of the *CGI-58* in another allele (compound heterozygous) or whether he harboured any posttransriptional alteration in this gene. Recent findings of the *CGI-58* gene expanded the clinical and mutational spectrum and underlie the genetic heterogeneity of this disease [21]. Alternatively, unknown mutations of other gene including the *ATGL* gene, might play a role [10], since mutations of *CGI-58* were not invariably found in clinically typical patients with DCS [15,17].

In the present study, a lipid analysis of scales from the DCS patient revealed elevated TG levels in the epidermis, which was correlated with the clinical severity of ichthyosis. A decrease in FFA levels in the epidermis could be also attributed to a dysfunction of ATGL in this patient. Since cholesterol, ceramides, and FFA comprise intercellular lipids of the stratum corneum, a decrease in FFA levels could affect the integrity of the cornified layer [22,23]. These abnormalities might contribute to development of ichthyosis in this patient. It is, however, unclear why permeability barrier remained intact in our patient, while the water holding capacity was markedly decreased in the involved lesions. Akiyama and coworkers recently demonstrated that CGI-58 knockdown reduced expression of keratinocyte differentiation markers including filaggrin [13], which plays an important role in retaining stratum corneum water.

New pieces of puzzle come from the finding of seasonal fluctuation of ichthyosis severity in this patient and a previous case [8], presumably depending on the environmental temperature. In both cases, summer was an aggravating season. Elevation of temperature might affect the ATGL activity, if any left, or other lipolysis pathways, for example, the hormone sensitive lipase-dependent pathway [18]. Therefore, it should be clarified how the mutated *CGI-58* in our patient impaired the ATGL, and whether ATGL, if any, or other compensatory lipase activity were temperature-sensitive. Haemmerle et al. have demonstrated that $ATGL^{-/-}$ mice showed defective cold adaptation because they could not produce FFAs to fuel thermogenesis [18]. We assume that ATGL activity could be decreased upon elevated environmental temperature because relatively reduced requirement of FFAs to be provided. In a patient like our case, impaired CGI-58 activity further might attenuate the ATGL activity at high temperature. To

verify this, lipase activity assay from the patient's cells will be required to see whether heat stimulation worsens it, which would be reversed by introduction of wild-type *CGI-58* gene.

Acknowledgments

We greatly thank Dr. Mikiro Takaishi and Ms. Reiko Kamijima for technical assistance, Drs. Ken Hashimoto, Walter M. Holleran, and Peter M. Elias for helpful discussion.

References

[1] Dorfman ML, Hershko C, Eisenberg S, Sagher F. Ichthyosiform dermatosis with systemic lipidosis. Arch Dermatol 1974;110:261–6.
[2] Chanarin I, Patel A, Slavin G, Wills EJ, Andrews TM, Stewart G. Neutral-lipid storage disease: a new disorder of lipid metabolism. Br Med J 1975;1:553–5.
[3] Elias PM, Williams ML. Neutral lipid storage disease with ichthyosis. Defective lamellar body contents and intracellular dispersion. Arch Dermatol 1985;121:1000–8.
[4] Rozenszajn L, Klajman A, Yaffe D, Efrati P. Jordans' anomaly in white blood cells. Report of case. Blood 1966;28:258–65.
[5] Pena-Penabad C, Almagro M, Martinez W, Garcia-Silva J, Del Pozo J, Yebra MT, et al. Dorfman–Chanarin syndrome (neutral lipid storage disease): new clinical features. Br J Dermatol 2001;144:430–2.
[6] Srebrnik A, Brenner S, Ilie B, Messer G. Dorfman–Chanarin syndrome: morphologic studies and presentation of new cases. Am J Dermatopathol 1998;20:79–85.
[7] Srebrnik A, Tur E, Perluk C, Elman M, Messer G, Ilie B, et al. Dorfman–Chanarin syndrome. A case report and a review. J Am Acad Dermatol 1987;17:801–8.
[8] Pujol RM, Gilaberte M, Toll A, Florensa L, Lloreta J, Gonzalez-Ensenat MA, et al. Erythrokeratoderma variabilis-like ichthyosis in Chanarin–Dorfman syndrome. Br J Dermatol 2005;153:838–41.
[9] Lefevre C, Jobard F, Caux F, Bouadjar B, Karaduman A, Heilig R, et al. Mutations in CGI-58, the gene encoding a new protein of the esterase/lipase/thioesterase subfamily, in Chanarin–Dorfman syndrome. Am J Hum Genet 2001;69:1002–12.
[10] Lass A, Zimmermann R, Haemmerle G, Riederer M, Schoiswohl G, Schweiger M, et al. Adipose triglyceride lipase-mediated lipolysis of cellular fat stores is activated by CGI-58 and defective in Chanarin–Dorfman syndrome. Cell Metab 2006;3:309–19.
[11] Yen CL, Farese Jr RV. Fat breakdown: a function for CGI-58 (ABHD5) provides a new piece of the puzzle. Cell Metab 2006;3:305–7.
[12] Yamaguchi T, Omatsu N, Matsushita S, Osumi T. CGI-58 interacts with perilipin and is localized to lipid droplets. Possible involvement of CGI-58 mislocalization in Chanarin–Dorfman syndrome. J Biol Chem 2004;279:30490–7.
[13] Akiyama M, Sakai K, Takayama C, Yanagi T, Yamanaka Y, McMillan JR, et al. CGI-58 is an alpha/beta-hydrolase within lipid transporting lamellar granules of differentiated keratinocytes. Am J Pathol 2008;173:1349–60.
[14] Akiyama M, Sawamura D, Nomura Y, Sugawara M, Shimizu H. Truncation of CGI-58 protein causes malformation of lamellar granules resulting in ichthyosis in Dorfman–Chanarin syndrome. J Invest Dermatol 2003;121:1029–34.
[15] Demerjian M, Crumrine DA, Milstone LM, Williams ML, Elia PM. Barrier dysfunction and pathogenesis of neutral lipid storage disease with ichthyosis (Chanarin–Dorfman syndrome). J Invest Dermatol 2006;126:2032–8.
[16] Ben Selma Z, Yilmaz S, Schischmanoff PO, Blom A, Ozogul C, Laroche L, et al. A novel S115G mutation of CGI-58 in a Turkish patient with Dorfman–Chanarin syndrome. J Invest Dermatol 2007;127:2273–6.
[17] Fischer J, Lefevre C, Morava E, Mussini JM, Laforet P, Negre-Salvayre A, et al. The gene encoding adipose triglyceride lipase (PNPLA2) is mutated in neutral lipid storage disease with myopathy. Nat Genet 2007;39:28–30.
[18] Haemmerle G, Lass A, Zimmermann R, Gorkiewicz G, Meyer C, Rozman J, et al. Defective lipolysis and altered energy metabolism in mice lacking adipose triglyceride lipase. Science 2006;312:734–7.
[19] Uchida Y, Behne M, Quiec D, Elias PM, Holleran WM. Vitamin C stimulates sphingolipid production and markers of barrier formation in submerged human keratinocyte cultures. J Invest Dermatol 2001;117:1307–13.
[20] Hashimoto K, Khan S. Harlequin fetus with abnormal lamellar granules and giant mitochondria. J Cutan Pathol 1992;19:247–52.
[21] Bruno C, Bertini E, Di Rocco M, Cassandrini D, Ruffa G, De Toni T, et al. Clinical and genetic characterization of Chanarin–Dorfman syndrome. Biochem Biophys Res Commun 2008;369:1125–8.
[22] Grubauer G, Feingold KR, Elias PM. Relationship of epidermal lipogenesis to cutaneous barrier function. J Lipid Res 1987;28:746–52.
[23] Mao-Qiang M, Elias PM, Feingold KR. Fatty acids are required for epidermal permeability barrier function. J Clin Invest 1993;92:791–8.

Acta Derm Venereol 2010; 90: 165–169

CLINICAL REPORT

Response of Intractable Skin Ulcers in Recessive Dystrophic Epidermolysis Bullosa Patients to an Allogeneic Cultured Dermal Substitute

Ken NATSUGA[1], Daisuke SAWAMURA[1], Maki GOTO[1], Erina HOMMA[1], Yuka GOTO-OHGUCHI[1], Satoru AOYAGI[1], Masashi AKIYAMA[1], Yoshimitsu KUROYANAGI[2] and Hiroshi SHIMIZU[1]

[1]Department of Dermatology, Hokkaido University Graduate School of Medicine, Sapporo, Japan, and [2]Regenerative Tissue Engineering, Graduate School of Medical Sciences, Kitasato University, Sagamihara, Japan

Recessive dystrophic epidermolysis bullosa (RDEB) is an inherited skin disorder caused by mutations in the *COL7A1* gene, which encodes collagen VII (COL7). Skin ulcers in RDEB patients are sometimes slow to heal. We describe here the therapeutic response of intractable skin ulcers in two patients with generalized RDEB to treatment with an allogeneic cultured dermal substitute (CDS). Skin ulcers in both patients epithelialized by 3–4 weeks after this treatment. Immunohistochemical studies demonstrated that the COL7 expression level remained reduced with respect to the control skin and that it did not differ significantly between graft-treated and untreated areas. Electron microscopy showed aberrant anchoring fibrils beneath the lamina densa of both specimens. In conclusion, CDS is a promising modality for treatment of intractable skin ulcers in patients with RDEB, even though it does not appear to increase COL7 expression. *Key words: epidermolysis bullosa; collagen VII; cultured dermal substitute; fibroblast; growth factor.*

(Accepted October 6, 2009.)

Acta Derm Venereol 2010; 90: 165–169.

Ken Natsuga, Department of Dermatology, Hokkaido University Graduate School of Medicine, North 15, West 7, Sapporo 060-8638, Japan. E-mail: natsuga@med.hokudai.ac.jp

Epidermolysis bullosa (EB) comprises a group of inherited bullous disorders that can be divided into three main phenotypes – epidermolysis bullosa simplex (EBS), junctional epidermolysis bullosa (JEB), and dystrophic epidermolysis bullosa (DEB) – depending on the level of skin cleavage (1). DEB is caused by mutations in the collagen VII gene (*COL7A1*), which encodes the main protein that forms anchoring fibrils beneath the dermal-epidermal junction (DEJ) (2). DEB is inherited as either autosomal dominant (DDEB) or recessive (RDEB) disease, each form having a different clinical presentation (2). Severe generalized RDEB (RDEB-sev gen) is characterized by a complete absence of collagen VII protein (COL7) from the DEJ and a total loss of anchoring fibrils ultrastructurally. A milder form of RDEB, generalized other RDEB (RDEB-O), always shows detectable but decreased COL7 expression at the DEJ. Patients with RDEB easily develop skin erosions at sites of trauma. These usually resolve spontaneously within several weeks, but occasionally lead to more persistent skin lesions or intractable ulcers.

Allogeneic tissues have been used to develop several therapeutic approaches for skin ulcers. Apligraf® (Organogenesis, Canton, MA, USA) is an allogeneic cultured skin substitute that consists of keratinocytes and fibroblasts supported on a scaffold (3). It is indicated for the treatment of venous ulcers (4). The application of Apligraf® to EB skin ulcers has been reported in approximately 30 cases thus far, with favourable results (5–7).

In parallel, Kubo & Kuroyanagi (8–11) have developed an allogeneic cultured dermal substitute (CDS) comprising a two-layered spongy matrix of hyaluronic acid and atelo-collagen containing fibroblasts. The efficacy of this CDS has been shown in animal models and some clinical trials (11–16). Recently, three patients with RDEB-sev gen were reported to have been treated successfully with CDS, although details regarding COL7 expression were not mentioned (17). Here, we confirm the efficacy of this CDS in the treatment of intractable skin ulcers in two RDEB-O patients, and we conducted immunohistochemical and ultrastructural investigation into whether the expression of COL7 is altered after this CDS treatment.

METHODS

Patients

Two patients with RDEB-O whose diagnosis was made by *COL7A1* mutation analysis and electron microscopy had persistent skin ulcers on their feet that failed to respond to supportive care for more than 6 months.

Preparation of allogeneic CDS

The CDS was prepared as described previously (9, 11). Briefly, an aqueous solution of hyaluronic acid (HA) with a cross-linking agent was frozen to –85°C in a dish and then lyophilized to obtain an HA sponge. The sponge was thoroughly rinsed with distilled water to remove free cross-linking agent,

then the hydrated HA sponge was frozen and lyophilized to obtain a purified HA sponge, which was immersed in a dish of atelo-collagen (AC) solution. Medical-grade AC was prepared by enzymatic cleavage of telopeptides on both ends of type I collagen molecules derived from porcine dermis. The hydrated HA sponge with AC was frozen and lyophilized to obtain a two-layered sponge of HA and AC. Both surfaces of the two-layered sponge were irradiated with an ultraviolet lamp to induce intermolecular cross-linking between AC molecules.

Cell banking was established as described previously (9, 11). The piece of skin used in this study was derived from a young donor who was free from infectious viruses such as hepatitis B and C (HBV and HCV), human immunodeficiency virus (HIV) and human T-lymphotropic virus (HTLV), and who tested negative in the treponema pallidum hemagglutination test (TPHA), in compliance with the ethical guidelines of St. Marianna University Graduate School of Medicine (Kanagawa, japan). Fibroblasts were isolated by enzymatic treatment. Cultivation of fibroblasts was initiated in culture medium to establish cell banking, as described (18). Viral infection of the cells, including HBV, HCV, HIV, HTLV and parvovirus, was excluded.

The fibroblasts cryopreserved in cell banking were thawed and cultured to obtain an adequate number of cells. These fibroblasts were seeded on a two-layered spongy matrix and cultured for one week. The number of fibroblasts seeded on the two-layered sponge was adjusted to 1.0×10^5 cells/cm^2. The resulting CDS was cryopreserved according to a previously described method (8, 19). Prior to clinical application, a polystyrene dish containing the CDS was placed in a foam polystyrene box at room temperature for 30 min and then floated in a water bath at 37°C.

Treatment regimens

After giving their informed consent, the patients received this CDS therapy. The surface of the designated skin ulcer was rinsed with saline solution. After thawing, then rinsing in lactated Ringer's solution, the CDS was applied to the wound surface, together with a gauze dressing to protect the CDS. The CDS was fixed with the bandage, and there were no restrictions on patient activity at any time after the CDS was in place. A new CDS was applied twice a week for the first 2 weeks and then once a week afterwards.

Immunofluorescence

Skin biopsies were taken from both patients under local anaesthesia from non-blistered and grafted skin areas after re-epithelialization. Follow-up biopsies were at 4 weeks (Patient 1) and 3 weeks (Patient 2) after the first CDS treatment, respectively, and one week after the last CDS application. The specimens were embedded in optimum cutting temperature (OCT) compound (Miles Scientific, Naperville, IL, USA). Immunofluorescence staining was performed on 5-micron cryosections of skin with the monoclonal antibody LH7:2 (recognizing the NC-1 domain of COL7) (20). To estimate the amount of COL7, serial dilution of LH7:2 was performed to 1:10, 1:20, 1:40, 1:80, 1:160, 1:320, 1:640 and 1:1280. Labelling was visualized using fluorescein isothiocyanate (*FITC*)-conjugated goat anti-mouse immunoglobulin (Ig)G.

Electron microscopy

Skin biopsies were taken from Patient 2 under local anaesthesia from the intact and grafted skin areas after complete epithelialization. Skin biopsy samples were fixed in 2% glutaraldehyde solution, post-fixed in 1% OsO_4, dehydrated, and embedded in Epon 812 (TAAB Laboratories Ltd, Aldermaston, Berkshire, UK). The samples were sectioned at 1 μm thickness for light microscopy and ultrathin sectioned for electron microscopy (at 70 nm thickness). The thin sections were stained with uranyl acetate and lead citrate and examined by transmission electron microscopy (Hitachi H7100, Hitachi, Tokyo, Japan).

CASE REPORTS

Patient 1

A 51-year-old female with RDEB-O had a history of three cutaneous squamous cell carcinomas (SCC), the details of which have been described elsewhere (21). *COL7A1* gene mutation analysis revealed that the patient was a compound heterozygote for c.5443G >A (p.G1815R) and c.5818delC (22, 23). She presented with an intractable ulcer, measuring 30 × 11 mm, on the back of her right foot, which had failed to respond to conservative, supportive therapy for 10 months (Fig. 1A). A skin biopsy specimen from the ulcer showed no findings suggestive of SCC. The CDS treatment was performed at site of the ulcer, and epithelialization of the lesion was observed within 4 weeks after the onset of treatment (Fig. 1B). Labelling of the DEJ in the patient's non-grafted and grafted skin samples with anti-COL7 antibody LH7:2 revealed no significant difference in the intensity of COL7 staining (Figs 2A, B). Both samples showed positive up to 1:160 dilution of the antibody as compared to 1:640 in normal skin (data not shown).

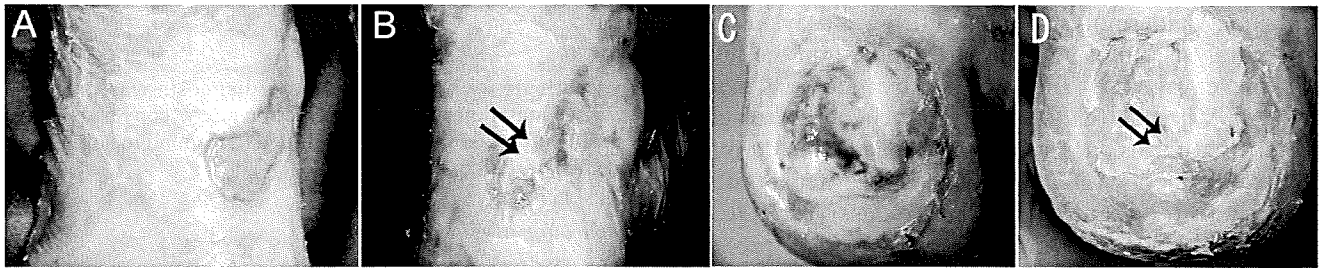

Fig. 1. Clinical response to allogeneic cultured dermal substitute (CDS) treatment (A). A skin ulcer measuring 30 × 11 mm on the back of the right foot in Patient 1. The ulcer had not healed for 10 months. (B) Re-epithelialization at 4 weeks after CDS treatment, although small erosions persist. (C) A skin ulcer measuring 21 × 20 mm on the right heel of Patient 2. The ulcer had persisted despite conservative treatment for 6 months. (D) Complete re-epithelialization 3 weeks after CDS treatment. The biopsy sites are indicated by arrows.

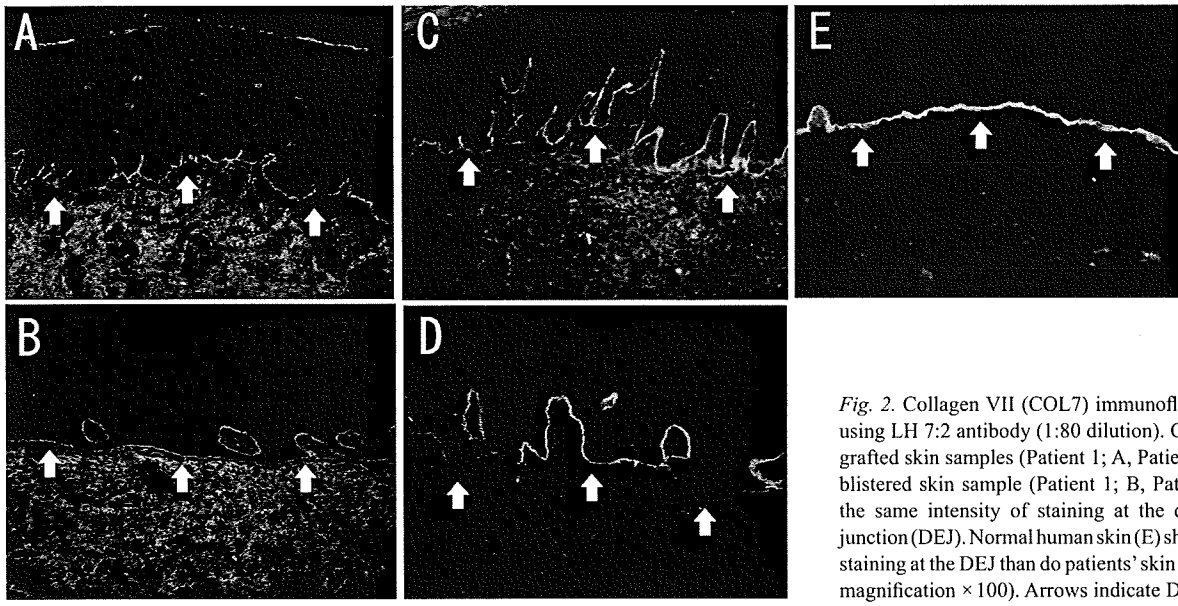

Fig. 2. Collagen VII (COL7) immunofluorescence study using LH 7:2 antibody (1:80 dilution). COL7 labelling in grafted skin samples (Patient 1; A, Patient 2; C) and non-blistered skin sample (Patient 1; B, Patient 2; D) shows the same intensity of staining at the dermal-epidermal junction (DEJ). Normal human skin (E) shows more intense staining at the DEJ than do patients' skin samples (original magnification × 100). Arrows indicate DEJ.

Patient 2

A 38-year-old female had been diagnosed with RDEB-O. She also had IgA nephropathy and was being treated with corticosteroids. DNA analysis revealed a recurrent *COL7A1* mutation c.5932C>T (p.R1978X) (23) and a novel mutation c.8029G>A (p.G2677S). She presented with a recalcitrant ulcer, measuring 21 × 20 mm, on her right heel, which had failed to respond to conservative therapy for the previous 6 months (Fig. 1C). Complete epithelialization of the lesion was observed 3 weeks after the beginning of CDS treatment (Fig. 1D). Labelling of the DEJ in the patient's non-blistered and grafted skin with LH7:2 revealed the same intensity of COL7 staining (Figs 2C, D). Both of the samples showed positive at the DEJ up to 1:320 dilution of the antibody (data not shown). Ultrastructurally, the anchoring fibrils from the patient's grafted skin samples were short, thin sub-lamina-densa structures (Fig. 3A) with the same features as those observed in the non-grafted skin samples (Fig. 3B).

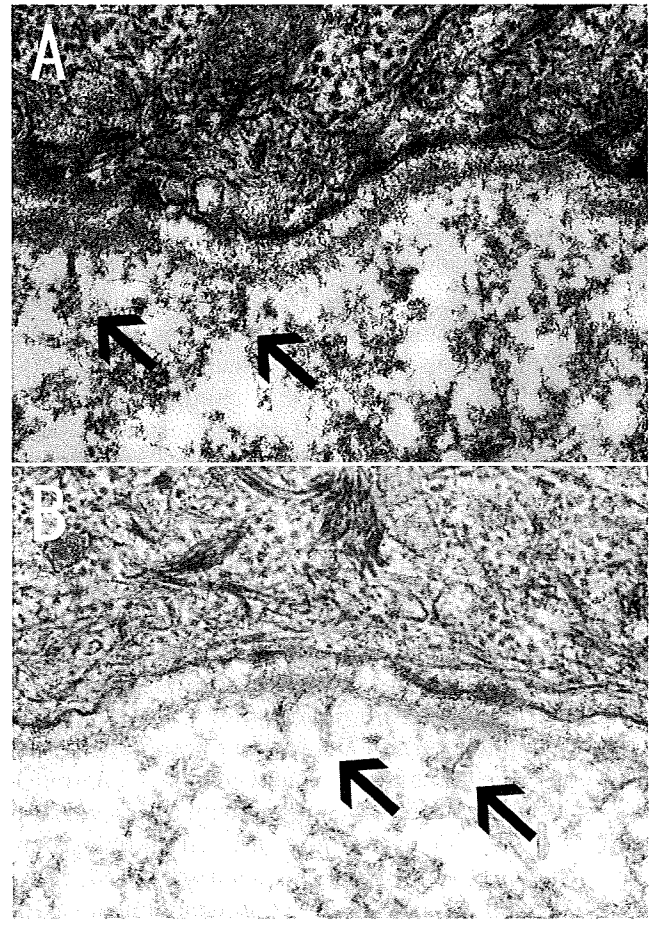

Fig. 3. Ultrastructural features of the sub-lamina densa region and basement membrane zone in the grafted and non-grafted skin of Patient 2. Discernible anchoring fibril-like structures (*arrows*) are observed beneath the lamina densa at the grafted skin site (A), as well as at the non-grafted skin site (B) (original magnification × 30,000).

DISCUSSION

Patients with EB have severe skin fragility and chronic wounding, which affect them physically and emotionally. Various controlled trials have been attempted with EB patients, including administration of phenytoin, topical bufexamac, aluminium chloride hexahydrate and oxytetracycline, although none of these has been uneqivocally successful (24). Experimental models of EB treatment have shown some promising results, but there are tremendous difficulties in translating such therapies into practical treatments for human patients (25). *Ex vivo* gene therapy for one patient with JEB

(26) and allogeneic cell therapy for patients with RDEB (27) have been described in the literature. Allogeneic tissue-engineered skin grafts have also been used for patients with RDEB. McGrath et al. (28) reported that cultured keratinocyte allografts did not significantly improve wound healing in 10 patients with RDEB. Apligraf®, a composite of cultured fibroblasts and keratinocytes, showed favourable results in 12 patients with RDEB (5, 6).

The main role of anchoring fibrils, of which COL7 is the main component, is in maintaining normal epidermal-dermal adherence between the basal lamina and the underlying superficial dermis. Besides this adhesive role, COL7 also aids and facilitates in the attachment and migration of keratinocytes and fibroblasts (29), and COL7 dysfunction can result in delayed wound healing (30). Indeed, COL7 staining is observed in the wound bed and neodermis in acute wound healing (31). This is the first study to assess COL7 expression of patients with RDEB after CDS treatment by immunofluorescence and electron-microscopy. In both of our cases, increased expression of COL7 after this CDS treatment could not be confirmed. Some technical difficulties in detecting a small increase in the protein could explain this result, because patients with RDEB-O who participated in this study expressed reduced but detectable amounts of COL7 in the baseline. It is also possible COL7 released from allogeneic fibroblasts could have been degraded in the wound bed instead of depositing at the DEJ.

The fibroblasts contained in the CDS release various cytokines and growth factors that play major roles in modulating wound healing. These cytokines and growth factors include vascular endothelial growth factor (VEGF), basic fibroblast growth factor (bFGF), hepatocyte growth factor (HGF), keratinocyte growth factor (KGF), platelet-derived growth factor (PDGF), transforming growth factor (TGF)-beta1, and interleukins (IL)-6 and IL-8 (32, 33). These cytokines and growth factors may have contributed to accelerated wound healing in our patients, although the cytokine levels in the skin samples were not assessed.

This study demonstrated that CDS treatment potentially benefits patients with RDEB-O. Former studies also demonstrated that intractable ulcers of patients with RDEB-sev gen improved after CDS treatment (17). An application of CDS without fibroblasts could be used as a negative control and would have improved our study. We have reported previously a comparative study of CDS with and without cultured fibroblasts on animal models (34). However, it is not always ethically easy to design a control study in human clinical trials. Furthermore, in our study, we selected two RDEB patients whose persistent foot ulcers failed to respond to supportive care for more than 6 months and there were no other similar foot ulcer for a comparative study.

The clinical improvement observed after CDS treatment is promising, and no restrictions on patient activity are needed. However, it is not practical to apply CDS to all ulcers of RDEB patients, because multiple ulcers are typically found on the whole body of RDEB. Intractable ulcers in RDEB patients, which do not respond to supportive care for several weeks, should be the main target of CDS treatment.

In conclusion, our study clearly demonstrates the efficacy of this CDS in the treatment of intractable skin ulcers in RDEB patients. Further examination to elucidate the mechanism of this treatment is required.

REFERENCES

1. Fine JD, Eady RA, Bauer EA, Bauer JW, Bruckner-Tuderman L, Heagerty A, et al. The classification of inherited epidermolysis bullosa (EB): report of the Third International Consensus Meeting on Diagnosis and Classification of EB. J Am Acad Dermatol 2008; 58: 931–950.
2. Varki R, Sadowski S, Uitto J, Pfendner E. Epidermolysis bullosa. II. Type VII collagen mutations and phenotype-genotype correlations in the dystrophic subtypes. J Med Genet 2007; 44: 181–192.
3. Eaglstein WH, Falanga V. Tissue engineering and the development of Apligraf a human skin equivalent. Adv Wound Care 1998; 11: 1–8.
4. Falanga V, Margolis D, Alvarez O, Auletta M, Maggiacomo F, Altman M, et al. Rapid healing of venous ulcers and lack of clinical rejection with an allogeneic cultured human skin equivalent. Human Skin Equivalent Investigators Group. Arch Dermatol 1998; 134: 293–300.
5. Fivenson DP, Scherschun L, Cohen LV. Apligraf in the treatment of severe mitten deformity associated with recessive dystrophic epidermolysis bullosa. Plast Reconstr Surg 2003; 112: 584–588.
6. Falabella AF, Valencia IC, Eaglstein WH, Schachner LA. Tissue-engineered skin (Apligraf) in the healing of patients with epidermolysis bullosa wounds. Arch Dermatol 2000; 136: 1225–1230.
7. Falabella AF, Schachner LA, Valencia IC, Eaglstein WH. The use of tissue-engineered skin (Apligraf) to treat a newborn with epidermolysis bullosa. Arch Dermatol 1999; 135: 1219–1222.
8. Kubo K, Kuroyanagi Y. Development of a cultured dermal substitute composed of a spongy matrix of hyaluronic acid and atelo-collagen combined with fibroblasts: cryopreservation. Artif Organs 2004; 28: 182–188.
9. Kubo K, Kuroyanagi Y. Development of a cultured dermal substitute composed of a spongy matrix of hyaluronic acid and atelo-collagen combined with fibroblasts: fundamental evaluation. J Biomater Sci Polym Ed 2003; 14: 625–641.
10. Kubo K, Kuroyanagi Y. Characterization of a cultured dermal substitute composed of a spongy matrix of hyaluronic acid and collagen combined with fibroblasts. J Artif Organs 2003; 6: 138–144.
11. Kubo K, Kuroyanagi Y. Spongy matrix of hyaluronic acid and collagen as a cultured dermal substitute: evaluation in an animal test. J Artif Organs 2003; 6: 64–70.
12. Hasegawa T, Suga Y, Mizoguchi M, Muramatsu S, Mizuno Y, Ogawa H, et al. An allogeneic cultured dermal substitute suitable for treating intractable skin ulcers and large skin defects prior to autologous skin grafting: three case reports.

J Dermatol 2005; 32: 715–720.
13. Kashiwa N, Ito O, Ueda T, Kubo K, Matsui H, Kuroyanagi Y. Treatment of full-thickness skin defect with concomitant grafting of 6-fold extended mesh auto-skin and allogeneic cultured dermal substitute. Artif Organs 2004; 28: 444–450.
14. Moroi Y, Fujita S, Fukagawa S, Mashino T, Goto T, Masuda T, et al. Clinical evaluation of allogeneic cultured dermal substitutes for intractable skin ulcers after tumor resection. Eur J Dermatol 2004; 14: 172–176.
15. Yamada N, Uchinuma E, Kuroyanagi Y. Clinical trial of allogeneic cultured dermal substitutes for intractable skin ulcers of the lower leg. J Artif Organs 2008; 11: 100–103.
16. Yonezawa M, Tanizaki H, Inoguchi N, Ishida M, Katoh M, Tachibana T, et al. Clinical study with allogeneic cultured dermal substitutes for chronic leg ulcers. Int J Dermatol 2007; 46: 36–42.
17. Hasegawa T, Suga Y, Mizoguchi M, Ikeda S, Ogawa H, Kubo K, et al. Clinical trial of allogeneic cultured dermal substitute for the treatment of intractable skin ulcers in 3 patients with recessive dystrophic epidermolysis bullosa. J Am Acad Dermatol 2004; 50: 803–804.
18. Hashimoto A, Kuroyanagi Y. Standardization for mass production of allogeneic cultured dermal substitute by measuring the amount of VEGF, bFGF, HGF, TGF-beta, and IL-8. J Artif Organs 2008; 11: 225–231.
19. Kubo K, Kuroyanagi Y. The possibility of long-term cryopreservation of cultured dermal substitute. Artif Organs 2005; 29: 800–805.
20. Leigh IM, Eady RA, Heagerty AH, Purkis PE, Whitehead PA, Burgeson RE. Type VII collagen is a normal component of epidermal basement membrane, which shows altered expression in recessive dystrophic epidermolysis bullosa. J Invest Dermatol 1988; 90: 639–642.
21. Tomita Y, Sato-Matsumura KC, Sawamura D, Matsumura T, Shimizu H. Simultaneous occurrence of three squamous cell carcinomas in a recessive dystrophic epidermolysis bullosa patient. Acta Derm Venereol 2003; 83: 225–226.
22. Sato-Matsumura KC, Yasukawa K, Tomita Y, Shimizu H. Toenail dystrophy with COL7A1 glycine substitution mutations segregates as an autosomal dominant trait in 2 families with dystrophic epidermolysis bullosa. Arch Dermatol 2002; 138: 269–271.
23. Sawamura D, Goto M, Yasukawa K, Sato-Matsumura K, Nakamura H, Ito K, et al. Genetic studies of 20 Japanese families of dystrophic epidermolysis bullosa. J Hum Genet 2005; 50: 543–546.
24. Langan SM, Williams HC. A systematic review of randomized controlled trials of treatments for inherited forms of epidermolysis bullosa. Clin Exp Dermatol 2009; 34: 20–25.
25. Aumailley M, Has C, Tunggal L, Bruckner-Tuderman L. Molecular basis of inherited skin-blistering disorders, and therapeutic implications. Expert Rev Mol Med 2006; 8: 1–21.
26. Mavilio F, Pellegrini G, Ferrari S, Di Nunzio F, Di Iorio E, Recchia A, et al. Correction of junctional epidermolysis bullosa by transplantation of genetically modified epidermal stem cells. Nat Med 2006; 12: 1397–402.
27. Wong T, Gammon L, Liu L, Mellerio JE, Dopping-Hepenstal PJ, Pacy J, et al. Potential of fibroblast cell therapy for recessive dystrophic epidermolysis bullosa. J Invest Dermatol 2008; 128: 2179–2189.
28. McGrath JA, Schofield OM, Ishida-Yamamoto A, O'Grady A, Mayou BJ, Navsaria H, et al. Cultured keratinocyte allografts and wound healing in severe recessive dystrophic epidermolysis bullosa. J Am Acad Dermatol 1993; 29: 407–419.
29. Goto M, Sawamura D, Nishie W, Sakai K, McMillan JR, Akiyama M, et al. Targeted skipping of a single exon harboring a premature termination codon mutation: implications and potential for gene correction therapy for selective dystrophic epidermolysis bullosa patients. J Invest Dermatol. 2006; 126: 2614–2620.
30. Chen M, Kasahara N, Keene DR, Chan L, Hoeffler WK, Finlay D, et al. Restoration of type VII collagen expression and function in dystrophic epidermolysis bullosa. Nat Genet 2002; 32: 670–675.
31. Haapasalmi K, Makela M, Oksala O, Heino J, Yamada KM, Uitto VJ, et al. Expression of epithelial adhesion proteins and integrins in chronic inflammation. Am J Pathol 1995; 147: 193–206.
32. Kubo K, Kuroyanagi Y. Effects of vascular endothelial growth factor released from cultured dermal substitute on proliferation of vascular endothelial cells in vitro. J Artif Organs 2003; 6: 267–272.
33. Kubo K, Kuroyanagi Y. A study of cytokines released from fibroblasts in cultured dermal substitute. Artif Organs 2005; 29: 845–849.
34. Tanaka M, Nakakita N, Kuroyanagi Y. Allogeneic cultured dermal substitute composed of spongy collagen containing fibroblasts: evaluation in animal test. J Biomater Sci Polym Ed 1999; 10: 433-453.

RESEARCH ARTICLE

Human Mutation

OFFICIAL JOURNAL

HGVS HUMAN GENOME VARIATION SOCIETY

www.hgvs.org

Plectin Expression Patterns Determine Two Distinct Subtypes of Epidermolysis Bullosa Simplex

Ken Natsuga,[1] Wataru Nishie,[1] Masashi Akiyama,[1] Hideki Nakamura,[1] Satoru Shinkuma,[1] James R. McMillan,[1] Akari Nagasaki,[1] Cristina Has,[1] Takeshi Ouchi,[3] Akira Ishiko,[3] Yoshiaki Hirako,[4] Katsushi Owaribe,[4] Daisuke Sawamura,[1] Leena Bruckner-Tuderman,[2,5] and Hiroshi Shimizu[1]*

[1]*Department of Dermatology, Hokkaido University Graduate School of Medicine, Sapporo, Japan;* [2]*Department of Dermatology, University Medical Center Freiburg, Germany;* [3]*Department of Dermatology, Keio University School of Medicine, Tokyo, Japan;* [4]*Division of Biological Science, Graduate School of Science, Nagoya University, Nagoya, Japan;* [5]*Freiburg Institute of Advanced Studies, School of Life Sciences, Freiburg, Germany*

Communicated by Peter H. Byers

Received 30 June 2009; accepted revised manuscript 8 December 2009.

Published online 5 January 2010 in Wiley InterScience (www.interscience.wiley.com). DOI 10.1002/humu.21189

ABSTRACT: Plectin is a cytoskeletal linker protein that has a dumbbell-like structure with a long central rod and N- and C-terminal globular domains. Mutations in the gene encoding plectin (*PLEC1*) cause two distinct autosomal recessive subtypes of epidermolysis bullosa (EB): EB simplex with muscular dystrophy (EBS-MD), and EB simplex with pyloric atresia (EBS-PA). Here, we demonstrate that normal human fibroblasts express two different plectin isoforms including full-length and rodless forms of plectin. We performed detailed analysis of plectin expression patterns in six EBS-MD and three EBS-PA patients. In EBS-PA, expression of all plectin domains was found to be markedly attenuated or completely lost; in EBS-MD, the expression of the N- and C-terminal domains of plectin remained detectable, although the expression of rod domains was absent or markedly reduced. Our data suggest that loss of the full-length plectin isoform with residual expression of the rodless plectin isoform leads to EBS-MD, and that complete loss or marked attenuation of full-length and rodless plectin expression underlies the more severe EBS-PA phenotype. These results also clearly account for the majority of EBS-MD *PLEC1* mutation restriction within the large exon 31 that encodes the plectin rod domain, whereas EBS-PA *PLEC1* mutations are generally outside exon 31.

Hum Mutat 31:308–316, 2010. © 2010 Wiley-Liss, Inc.

KEY WORDS: *PLEC1*; basement membrane zone; skeletal muscle; mRNA decay; truncation

Introduction

Plectin is a 500-kDa intermediate filament-binding protein that serves as a crosslinking element of the cytoskeleton to supply mechanical strength to cells and tissues [Wiche, 1998]. Plectin is expressed in a wide variety of tissues, including skin, striated muscle, and gastrointestinal tract epithelia. Within the cutaneous epithelium, plectin is especially concentrated along the basal pole of basal keratinocytes, where it functions as a linker between the keratin intermediate filament cytoskeleton, hemidesmosomes, and the underlying basement membrane zone (BMZ) [Borradori and Sonnenberg, 1999]. Plectin interacts with α6 and β4 integrins [Geerts et al., 1999; Litjens et al., 2003, 2005; Niessen et al., 1997a,b; Rezniczek et al., 1998; Schaapveld et al., 1998], BPAG2 [Koster et al., 2003], and periplakin [Boczonadi et al., 2007].

Epidermolysis bullosa (EB) comprises a group of heterogeneous disorders in which congenital skin fragility leads to dermal–epidermal junction separation. EB is subdivided into the three major groups of EB simplex, junctional EB, dystrophic EB, and the one minor group of Kindler syndrome, based on the level of blister formation [Fine et al., 2008]. So far, mutations in 13 different genes have been identified as underlying EB subtypes [Fine et al., 2000, 2008]. Among them, mutations in the gene encoding plectin, *PLEC1* (MIM# 601282), are responsible for two distinct types of autosomal recessive EBS (EBS with muscular dystrophy [EBS-MD] and EBS with pyloric atresia [EBS-PA]) and one subtype of autosomal dominant EBS (EBS-Ogna) [Fine et al., 2008]. Patients with EBS-Ogna are heterozygous for one amino acid substitution in the rod domain of plectin [Koss-Harnes et al., 2002]. EBS-Ogna is thought to be caused by plectin perturbation that results from dominant negative interference [Pfendner et al., 2005]. In contrast, homozygous or compound heterozygous loss-of-function mutations in *PLEC1* lead to EBS-MD or EBS-PA.

EBS-MD is characterized by generalized blistering and delayed onset of muscular dystrophy. Defective expression of plectin was found in patients with EBS-MD [Gache et al., 1996] and mutations in *PLEC1* were found to be responsible for the EBS-MD phenotype [McLean et al., 1996; Smith et al., 1996]. To date, more than 30 EBS-MD patients have been reported to have *PLEC1* mutations [Bauer et al., 2001; Chavanas et al., 1996; Dang et al., 1998; Koss-Harnes et al., 2004; Kunz et al., 2000; McMillan et al., 2007; Mellerio et al., 1997; Pfendner et al., 2005; Pulkkinen et al., 1996; Rouan et al., 2000; Sawamura et al., 2007; Takahashi et al., 2005; Takizawa et al., 1999]. Most reported *PLEC1* mutations in EBS-MD patients are located within exon 31 encoding the large rod domain of plectin [Pfendner et al., 2005; Sawamura et al., 2007]. In contrast to the phenotype seen in EBS-MD, clinical manifestations of EBS-PA are more severe and are characterized by more generalized blistering and pyloric atresia,

Additional Supporting Information may be found in the online version of this article.

*Correspondence to: Hiroshi Shimizu, Department of Dermatology, Hokkaido University Graduate School of Medicine, North 15 West 7, Sapporo 060-8638, Japan. E-mail: shimizu@med.hokudai.ac.jp

which frequently leads to early death in affected patients. Similarly, junctional EB with pyloric atresia (JEB-PA) has been known to be caused by the mutation in the gene encoding α6/β4 integrin (*ITGA6*; MIM# 147556; *ITGB4*; MIM# 147557), and about 60 *ITGA6* or *ITGB4* mutations have been described [Fine et al., 2008; Varki et al., 2006]. Recently, our group and others identified *PLEC1* mutations in eight patients with EBS-PA [Nakamura et al., 2005; Pfendner et al., 2005; Pfendner and Uitto, 2005; Sawamura et al., 2007]. EBS-MD and EBS-PA represent distinct clinical phenotypes, although both are caused by *PLEC1* mutations. The exact mechanisms that produce the clinical differences between EBS-MD and EBS-PA subtypes have not been elucidated, although it has been postulated that the severity of EBS patients with *PLEC1* mutations could be associated with alternative splicing of plectin [Sawamura et al., 2007; Sonnenberg and Liem, 2007].

The present study demonstrates that normal human fibroblasts express two different plectin isoforms: full-length plectin, and a shorter rodless plectin. In light of this finding, we collected skin samples and cultured cells from patients with EBS-MD and EBS-PA in which we precisely analyzed their expression levels of plectin using immunoblotting, immunofluorescence, and semiquantitative RT-PCR to determine the different pathogenic mechanisms underlying *PLEC1* mutations. Our data suggest that EBS-MD and EBS-PA exhibit different plectin expression patterns, and this study gives further insight toward improving our understanding of genotype-phenotype correlation in EBS patients with *PLEC1* mutations.

Materials and Methods

Patients and Mutation Detection

Nine EBS patients in whom *PLEC1* mutations had been confirmed were analyzed: six EBS-MD and three EBS-PA unrelated individuals (Table 1). *PLEC1* mutations in four EBS-MD and three EBS-PA cases were previously described in the literature [Kunz et al., 2000; Nakamura et al., 2005; Pulkkinen et al., 1996; Sawamura et al., 2007; Takizawa et al., 1999]. Patients EBS-MD1 and EBS-MD5 were newly identified cases in the present study.

EBS-MD1 was a 24-year-old Japanese female. She was the first child of nonconsanguineous, healthy parents. Generalized blistering and erosions of the skin were noted at birth, together with nail dystrophy. She had no history of pyloric atresia. At the age of 10, she developed muscular dystrophy. EBS-MD5 was a 7-year-old Croatian male. He was the second child of nonconsanguineous, healthy parents. His elder brother was healthy. He developed generalized blistering, including of the oral mucosal, and laryngeal stridor, immediately after birth. Pyloric atresia was not observed. To date, he has not developed muscular dystrophy.

Genomic DNA (gDNA) was isolated from peripheral blood leukocytes (EBS-MD1 and her parents) or cultured fibroblasts (EBS-MD5). The mutation detection was performed after polymerase chain reaction (PCR) amplification of all *PLEC1* exons and intron–exon borders, followed by direct automated sequencing using an ABI PRISM 3100 genetic analyzer (Applied Biosystems, Foster City, CA). Oligonucleotide primers and PCR conditions used in this study were derived from a previous report [Nakamura et al., 2005]. The gDNA nucleotides, the complementary DNA (cDNA) nucleotides, and the amino acids of the protein, were numbered based on the previous sequence information (GenBank accession no. AH003623) [McLean et al., 1996].

The medical ethical committees of Hokkaido University, Keio University, and University Medical Center Freiburg approved all described studies. The study was conducted according to The Declaration of Helsinki Principles. Participants gave their written informed consent.

A schematic of plectin structure and *PLEC1* mutations detected in EBS patients in this study is shown in Figure 1A.

Antibodies

The plectin domains where the antibodies used in this study react are summarized in Figure 1B. Mouse monoclonal antibodies (mAbs), PN643 against the actin-binding domain of plectin and PC815 against the C-terminal plectin repeats were prepared by immunizing mice with recombinant His-tagged fusion proteins. To produce recombinant proteins, the cDNAs that encode the actin-binding domain of plectin and C-terminal plectin repeats comprising amino acids 171–595 and 2,930–3,153 (GenBank accession no. AAB05428.1), respectively, were cloned into a pET32c vector. The resultant recombinant proteins were expressed in the *Escherichia coli* expression host BL21(DE3)pLysS and purified using a His-Bind column (Novagen, Madison, WI). Spleen cells derived from immunized mice were fused with mouse myeloma cells. Hybridomas producing antibodies against plectin were selected by immunofluorescent microscopy screening using normal human skin. Immunoblotting using cytoplasmic extracts from DJM-1 cells confirmed that both of the antibodies reacted with a 500-kDa protein.

In addition to PN643 and PC815, the following mAbs against BMZ components were used: mAbs HD1-121 [Hieda et al., 1992; Okumura et al., 1999], 10F6 [Foisner et al., 1991], and 5B3 [Foisner et al., 1994] against the rod domain of plectin; mAb LH7.2 (Sigma, St. Louis, MO) against type VII collagen. mAb 10F6 and 5B3 were kind gifts from Dr. G. Wiche of the University of Vienna. C20, a goat polyclonal antibody against the C-terminus

Table 1. EBS Patients and *PLEC1* Mutations

Patient	Mutation 1 (predicted consequence)	Exon	Mutation 2 (predicted consequence)	Exon	Reference
EBS-MD1	**c.6549_6582del (p. Ala2183fs)**	31	**c.13040dup (p.Gly4347fs)**	32	Present case
EBS-MD2	c.4348C>T (p.Gln1450X)	31	c.4348C>T (p.Gln1450X)	31	Sawamura et al., 2007
EBS-MD3	c.3157C>T (p.Gln1053X)	24	c.5806C>T (p.Gln1936X)	31	Takizawa et al., 1999
EBS-MD4	c.5866del (p.Leu1956fs)	31	c.5866del (p.Leu1956fs)	31	Pulkkinen et al., 1996
EBS-MD5	**c.4643_4667dup (p.Arg1556fs)**	31	**c.7120C>T (p.Gln2374X)**	31	Present case
EBS-MD6	c.5188C>T (p.Gln1713X)	31	c.7102C>T (p.Arg2351X)	31	Kunz et al., 2000
EBS-PA1	c.7396C>T (p.Gln2466X)	31	c.7633C>T (p.Gln2545X)	32	Sawamura et al., 2007
EBS-PA2	c.3565C>T (p.Arg1189X)	27	c.7612C>T (p.Gln2538X)	32	Nakamura et al., 2005
EBS-PA3	c.913C>T (p.Gln305X)	9	c.1344G>A (p.Gln447fs; =)[a]	12	Nakamura et al., 2005

The novel *PLEC1* mutations detected in this study are in bold. MD, Muscular dystrophy; del, deletion; dup, duplication; fs, frameshift.
[a]The mutation c.1344G>A is at the 3′ end of exon12. Predicted consequences resulting from this mutation are discussed in the Results.

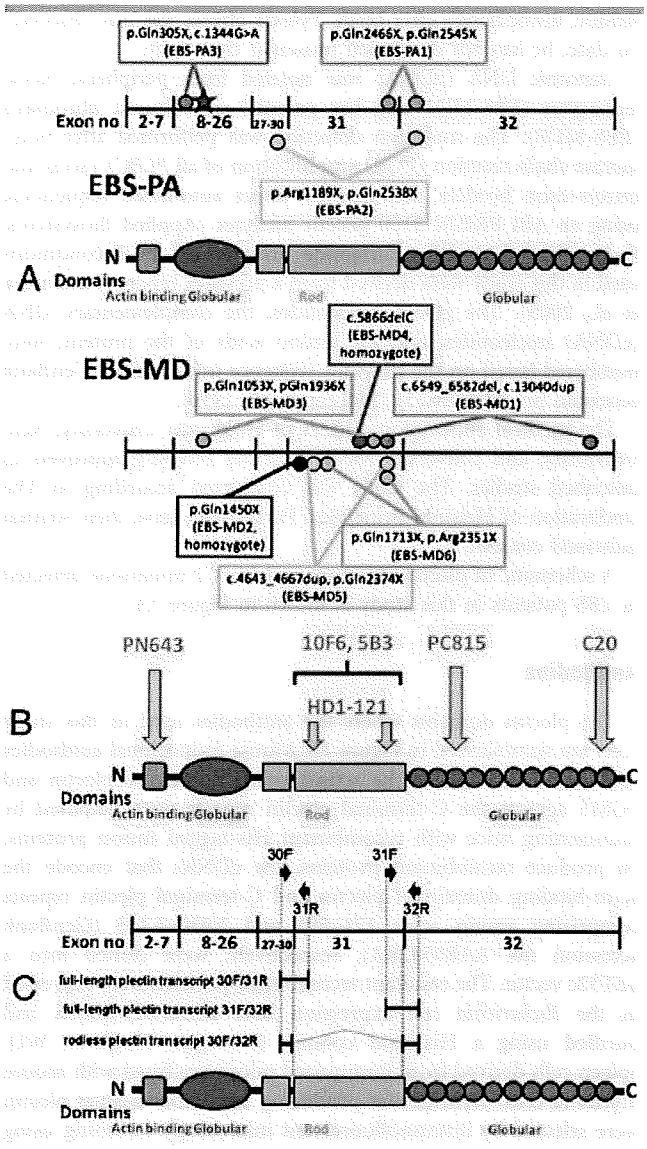

Figure 1. Scheme of plectin structure, PLEC1 mutations, antibodies against plectin and specific primers to detect the rodless transcript form of plectin. **A:** Plectin molecules consist of a central rod flanked by amino-terminal and carboxy-terminal globular domains. PLEC1 mutations observed in EBS patients of this study are indicated. Dots represent truncated mutations. The star indicates a splice-site mutation (c.1344G>A). **B:** PN643 is a monoclonal antibody (mAb) against the N-terminal actin-binding domain of plectin. HD1-121, 10F6, and 5B3 are mAbs against the rod domain of plectin. PC815 is a mAb and C20 is a polyclonal antibody against the C-terminal globular domain of plectin. **C:** Specific primers used to detect the presence of transcripts for full-length (30F/31R and 31F/32R) and rodless plectin (30F/32R) on cDNA synthesized from the mRNA of normal human, EBS-MD5 and EBS-PA3F cells.

of plectin, was purchased from Santa Cruz (Santa Cruz, CA). Anti-beta-actin mAb (AC15, Sigma) was used to confirm equal protein loading.

Immunofluorescence Studies

Immunofluorescence analysis was performed using skin specimens from the patients (Table 1). Fresh-frozen skin specimens were embedded in optimal cutting temperature (OCT) compound and quickly frozen in isopentane cooled over liquid nitrogen. 5-μm cryostat-cut sections were incubated overnight at 4°C with primary antibodies including the following mAbs: PN643 (working dilution of 1:160), HD1-121 (1:100), 10F6 (1:10), 5B3 (1:20), PC815 (1:20), and LH7.2 (1:10). After washing in phosphate-buffered saline, the sections were incubated with secondary antibodies conjugated with fluorescein-isothiocyanate.

Cell Culture and Immunoblot Analysis

Cultured fibroblasts were obtained from skin biopsies of a normal human volunteer and of patient EBS-MD5. Cultured amniocytes were derived from an aborted fetus who was a sibling of EBS-PA3 (EBS-PA3F). Prenatal diagnosis of EBS-PA3F revealed that the fetus had the same *PLEC1* mutations as were detected in EBS-PA3 (data not shown). Cultured fibroblasts and amniocytes were maintained in Dulbecco's modified Eagle's medium supplemented with 10% (v/v) fetal bovine serum. Cultured oral keratinocytes were obtained from biopsies of a normal human volunteer and were maintained in CnT-57 medium (CELLnTEC). Whole-cell lysates of human skeletal muscle were purchased from Abcam (ab82589). For sample preparation, cultured cells were lysed in Nonidet-40 (NP-40) containing buffer (1% NP-40, 25 mM Tris-HCl [pH 7.6], 4 mM EDTA, 100 mM NaCl, 1 mM phenylmethylsulfonyl fluoride [PMSF], and proteinase inhibitor cocktail [Sigma]) on ice for 30 min; cell debris was removed by centrifugation at 14,000 rpm for 15 min; and supernatant was collected. Supernatants were solubilized in Laemmli's sample buffer [Laemmli, 1970], applied to SDS-polyacrylamide gels, and transferred to a PVDF membrane. The membrane was incubated with PN643, HD1-121, C20, and AC15 overnight at 4°C followed by incubation with horseradish peroxidase (HRP) conjugated anti-mouse IgG (for PN643, HD1-121, and AC15) and HRP-conjugated antigout IgG (for C20) for 1 hr at room temperature. The blots were detected using ECL Plus Detection Kit (GE Healthcare, Fairfield, CT). The images were obtained with LAS-4000 mini (Fujifilm, Tokyo, Japan). To elucidate the quantitative ratio of full-length/rodless plectin, immunoblotting of lysates from normal human fibroblasts, keratinocytes, and skeletal muscle was performed in triplicate. Band intensities were analyzed by densitometry (ImageJ).

Semiquantitative RT-PCR Analysis

Total RNA was isolated from cultured fibroblasts (normal human volunteers and EBS-MD5) or amniocytes (EBS-PA3F) using RNeasy kit (Qiagen, Valencia, CA), and first-strand cDNA was made using Superscript II reverse transcriptase (Invitrogen, Carlsbad, CA). First-strand cDNA was then amplified by PCR with primers specific for the exon boundaries flanking the rod domain of plectin as described previously [Koster et al., 2004] (Fig. 1C). The following primers were used in this study: 30F, 5′-CATCAGCGAGACTCTGCGGC-3′; 31R, 5′-TGCGCCTGTCG-CTTTTGTGC-3′; 31F, 5′-AGCTGGAGATGAGCGCTGA-3′; 32R, 5′-TGCTGCAGCTCCTCCTGC-3′. PCR conditions were as follows: 94°C for 5 min, followed by 30 cycles (31F/32R, 30F/32R) and 35 cycles (30F/31R) at 94°C for 1 min, 62°C for 1 min, and 72°C for 1 min, and extension at 72°C for 7 min. To ensure equal loading, a housekeeping gene (GAPDH) was simultaneously amplified. The PCR products were assessed on a 2% agarose gel. The images were obtained with LAS-4000 mini (Fujifilm). To confirm the skipping of exon 31 in rodless transcript, direct sequencing was performed for the PCR products (30F/32R). To analyze transcripts derived from the c.1344G>A mutant allele,

PCR amplification of synthesized EBS-PA3F cDNA from exon 9 to exon 14 was performed using the following primers: 5′-GATTGAGATCCTGTGGTCTC-3′ and 5′-CTCTGCACACTCT-GCAGAGT-3′. PCR products were cloned in the TA cloning vector pCRII (Invitrogen) and then sequenced.

Results

PLEC1 Mutation Detection

PLEC1 mutational analysis in case EBS-MD1 demonstrated that the affected patient was a compound heterozygote for the maternal c.13040dup mutation in exon 32 and the paternal c.6549_6582del mutation in exon 31 (Supp. Fig. 1A). Both of the mutations resulted in a frameshift that caused 8- and 21-amino-acid missense sequences, respectively, followed by a premature termination codon (PTC). These mutations were novel, and they were confirmed by *Mwo*I restriction enzyme digestion and TA-cloning, respectively (data not shown). In addition, the c.10453C>T (p.Arg3485Trp) transition in exon 32 was also detected in one allele of the patient and her mother. This c.10453C>T transition was not found by sequence analysis in 100 normal unrelated Japanese alleles (50 healthy unrelated Japanese individuals), and it was unlikely to be polymorphism, although the contribution of this missense mutation to the EB phenotype remains unclear.

EBS-MD5 was a compound heterozygote for the c.4643_4667dup and c.7120C>T (p.Gln2374X) mutations in exon 31 (Supp. Fig. 1B). The c.4643_4667dup resulted in a frameshift that caused a 90-amino-acid missense sequence, followed by a PTC. These mutations were also novel and were confirmed by TA-cloning and *Pst*I restriction enzyme digestion respectively (data not shown).

Differential plectin isoform expression by immunoblotting in normal human fibroblasts

Immunoblot analysis of lysates from normal human cultured fibroblasts revealed that two closely spaced bands, putatively corresponding to two forms of plectin (500 kDa full-length and 390 kDa rodless form) reacted with PN643 and C20, antibodies recognizing the N- and C-termini of plectin (Fig. 2). Using HD1-121, an antibody against the rod domain of plectin, lysates from normal human fibroblasts reacted only with full-length plectin (Fig. 2). These results showed that normal human fibroblasts expressed two different *PLEC1* isoforms: full length and a shorter rodless plectin isoforms.

The Quantitative Ratio of Full-length/Rodless Plectin in Normal Human Fibroblasts, Keratinocytes, and Skeletal Muscle

To elucidate the relative amount of full-length and rodless plectin in normal human fibroblasts, keratinocytes, and skeletal muscle, we performed immunoblot analysis of lysates from each sample using PN643, an antibody against the N-terminus of plectin. Both full-length and rodless plectin were detected in each sample (Fig. 3). Band intensities were measured in triplicate ±SD. The quantitative ratio of full-length/rodless plectin was 14.2±4.2 in fibroblasts, 21.3±6.4 in keratinocytes, and 1.37±0.23 in skeletal muscle.

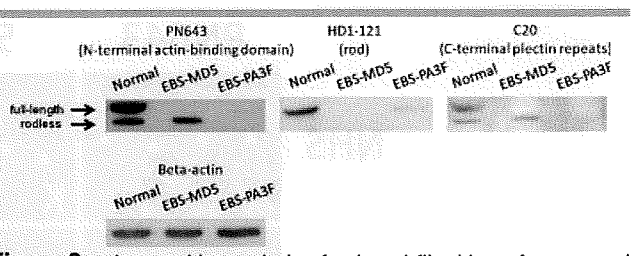

Figure 2. Immunoblot analysis of cultured fibroblasts from normal human control and EBS-MD and amniocytes from EBS-PA. Immunoblot analysis of extracts from cells of normal control, EBS-MD5, and an aborted sibling of EBS-PA3 (EBS-PA3F). Analysis used PN643 against the N-terminal actin-binding domain, HD1-121 against the rod domain and C20 against the C-terminal plectin repeats. Rodless plectin, detected with PN643 and C20, migrates just below full-length plectin in normal human fibroblasts. Using HD1-121, only full-length plectin was demonstrated in the normal control. In contrast, EBS-MD5 fibroblasts contained only rodless plectin, which was detected with PN643 and C20. Full-length plectin did not appear in EBS-MD5 using any antibody. EBS-PA3F amniocytes contained a greatly reduced amount of full-length plectin. Equal protein loading was confirmed by reprobing with AC15 (anti-beta-actin antibody). [Color figure can be viewed in the online issue, which is available at www.interscience.wiley.com.]

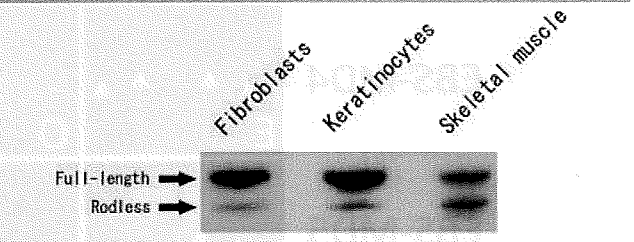

Figure 3. Relative amounts of full-length and rodless plectin in normal human fibroblasts, keratinocytes and skeletal muscle. Immunoblot analysis of lysates from normal human fibroblasts, oral keratinocytes, and skeletal muscle using PN643 against the N-terminal actin-binding domain of plectin was performed. Both full-length and rodless plectin were detected in each sample. The quantitative ratio of the two isoforms was calculated, using Image J software, as follows: 14.2±4.2 in fibroblasts, 21.3±6.4 in keratinocytes, and 1.37±0.23 in skeletal muscle. [Color figure can be viewed in the online issue, which is available at www.interscience.wiley.com.]

Characterization of cutaneous plectin expression patterns in EBS-MD and EBS-PA patients by immunofluorescence analysis

To assess whether expression patterns of plectin in the skin differ between EBS-MD and EBS-PA, we performed immunofluorescence analysis using five different antibodies (Fig. 1B). PN643 weakly reacted with skin specimens from all EBS-MD patients and two out of three EBS-PA patients (EBS-PA1, 3), but failed to react with specimens from EBS-PA2 (Fig. 4A–J). HD1-121 showed weakly reactivity in three EBS-MD patients (EBS-MD1, 4, 6) and one EBS-PA patient (EBS-PA3), but was negative in the other patients (EBS-MD2, 3, 5, EBS-PA1, 2) (data not shown). 5B3, the mAb against the rod domain of plectin, was faint but identifiable in two EBS-MD patients (EBS-MD1, 6) and one EBS-PA patient (EBS-PA3), but was negative in the other patients (EBS-MD2-5, EBS-PA1, 2) (Fig. 4L–T). No skin specimens reacted with 10F6, a monoclonal antibody against the rod domain, except EBS-PA3 (data not shown). PC815 recognized the C-terminus of plectin weakly but detectably in all EBS-MD patients and EBS-PA3, but not in EBS-PA patients 1 and 2 (Fig. 4V–AD). These results